Table 1. Vitamin and Mineral Composition of Royal Jelly Products (mg/100 g)

Components	Royal Jelly	Protease-Treated Royal Jelly
Minerals		
Sodium	40.2	2050
Phosphorus	662	580
Iron	3.21	2.8
Calcium	40.6	44.8
Potassium	814	766
Magnesium	90.9	74.3
Copper	1.34	0.91
Zinc	6.61	5.62
Manganese	0.22	0.17
Selenium	>0.005	0.006
Vitamins		
Thiamine	0.96	0.84
Riboflavin	2.03	1.92
Vitamin B6	1.12	0.63
α-Tocopherol	0.1	>0.1
Folic acid	0.12	0.06
Pantothenic acid	12.8	14.5
Biotin	0.0467	0.0722
Inositol	>2	41
Niacin	14.8	15.4
Choline	620	480

TA muscles were isolated, frozen in 2-methylbutane precooled in liquid nitrogen, and stored at −80°C for following histological analysis (26).

Measurements of Muscle Weight and Isolation of Satellite Cells

The satellite cells were isolated according to a previous study (6) with some modifications. The large hindlimb muscles of mice including the TA muscle, triceps surae muscle, quadriceps muscle, biceps femoris muscle, gluteus maximus muscle, and iliopsoas muscle were isolated, and the weights of the muscles were measured. Next, nonmuscle tissues were removed under a dissection microscope; the muscles were subjected to enzymatic dissociation with 0.2% collagenase Type II (Worthington Biochemical Corporation, Lakewood, NJ) for 60 minutes and then with 0.04 U/mL dispase (Gibco BRL, Grand Island, NY) for 45 minutes. The cell suspension was filtered through a cell strainer (BD Bioscience, Franklin Lakes, NJ), incubated with antimouse CD16/CD32 monoclonal antibody (mAb, 2.4G2, BD Bioscience) to block Fc receptors and then with the following antibodies: fluorescein isothiocyanate–labeled anti-CD31, anti-CD45 (BD Bioscience), anti-CD11b, and anti-Sca-1 antibodies (eBioscience, San Diego, CA); PE-labeled anti-integrin-α7 (MBL, Nagoya, Japan); and Alexa 647-labeled anti-CD34 (BD Bioscience). The cells were counted and sorted by FACSAria II flow cytometer (BD Bioscience) as previously shown (27).

Immunohistochemistry and Immunocytochemistry

Frozen muscle tissues were sectioned from a region approximately 3 mm from the top of the TA muscle (8 μm in thickness) using a cryostat. For embryonic myosin heavy chain (eMyHC) staining, frozen sections or cultured cells were fixed with acetone/methanol (50%/50%) for 30 seconds at −20°C. Specimens were blocked with 1% bovine serum albumin and 0.1% Triton X-100 in PBS at room temperature for 45 minutes and then incubated with anti-eMyHC antibody (F1.652, DSHB, Iowa City, IA) at 1:2 dilution at 4°C overnight, followed by Rodamine-conjugated secondary antibody staining (Chemicon International, Temecula, CA) at room temperature in the dark for 1 hour. For PAX7 staining, cultured cells were fixed with PBS containing 4% paraformaldehyde at room temperature for 20 minutes and then blocked with 1% bovine serum albumin and 0.1% Triton X-100 in PBS at room temperature for 45 minutes. After blocking, the cells were incubated with anti-Pax-7 antibody (R&D Systems, Minneapolis, NE) at 1:50 dilution at 4°C overnight followed by Alexa 488–coupled antimouse IgG antibody (Invitrogen) at 1:200 dilution at room temperature for 1 hour. Finally, the sections or cells were mounted in Vectashield Mounting Medium with 4′,6-diamidino-2-phenylindole (DAPI) (Vector labs, Burlingame, CA). In vivo, the regenerating capacity of the injured skeletal muscles was evaluated by quantifying the percentage of eMyHc-immunoreactive area per field (28). Ten randomly selected fields at ×200 magnification were measured in each sample. ImageJ software was used to quantify the eMyHC-immunoreactive areas per field. In vitro, the degree of differentiation of satellite cells of the aged mice was evaluated by the maximum diameter of the cells by Adobe Photoshop CS2 software (San Jose, CA). The muscle sections were stained for hematoxylin and eosin also. Images were taken using a phase-contrast and fluorescence microscope BZ9000 (Keyence, Osaka, Japan) (29).

Western Blot Analysis

PAX7, Type I IGF receptor (IGF-IR), Akt, and phosphorylated Akt (phospho-Akt) proteins were detected by Western blot analysis. In brief, the cells were rinsed twice with ice-cold PBS and lysed using RIPA Lysis Buffer (Upstate, Temecula, CA). The extracted protein fraction was electrophoresed in a sodium dodecyl sulfate and 10% polyacrylamide gel and then transferred onto an Immobilon transfer membrane (Millipore, Bedford, MA). The amount of protein loaded onto the gels was 36 μg per well. The membranes were immunoblotted with the primary antibodies to PAX7 (DSHB) at 1:100 dilution, GAPDH, IGF-IR, Akt, and phospho-Akt (Cell Signaling, Boston, MA) at 1:1000 dilution. Then, the membranes were incubated with horseradish peroxidase–conjugated antirabbit immunoglobulin G (Cell Signaling) at 1:25,000 dilution, and the protein bands were detected with an

enhanced chemiluminescence detection kit (Amersham, Buckinghamshire, UK) (30).

Enzyme-Linked Immunosorbent Assay

After RJ/pRJ treatment, the mice were anesthetized with diethyl ether, and blood samples were isolated from the inferior vena cava. The serum levels of interleukin-1α (IL-1α), IL-1β, IL-6, tumor necrosis factor-α, and IGF-1 were measured using a specific ELISA kit (R&D Systems) according to the manufacturer's instructions, respectively (22).

Statistical Analysis

Data are presented as mean ± standard deviation. Differences were analyzed by one-way analysis of variance test (Post hoc, Tukey). A level of $p < 0.05$ was accepted as statistically significant. All in vitro experiments were repeated at least three times.

Results

Isolation and Characterization of Satellite Cells

As an initial step, we tried to identify the effect of RJ/pRJ on satellite cells. The characterization of satellite cells by cell surface markers has been established only very recently (6). Therefore, according to that study, we first tried to isolate satellite cells with some modifications. We enzymatically dissociated mononuclear cells from the mouse hind-limb muscles (Figure 1A, circle: upper muscles were isolated from a right leg, and lower muscles were isolated from a left leg, from left to right, TA, triceps surae, quadriceps, divided biceps femoris into two, gluteus maximus, and

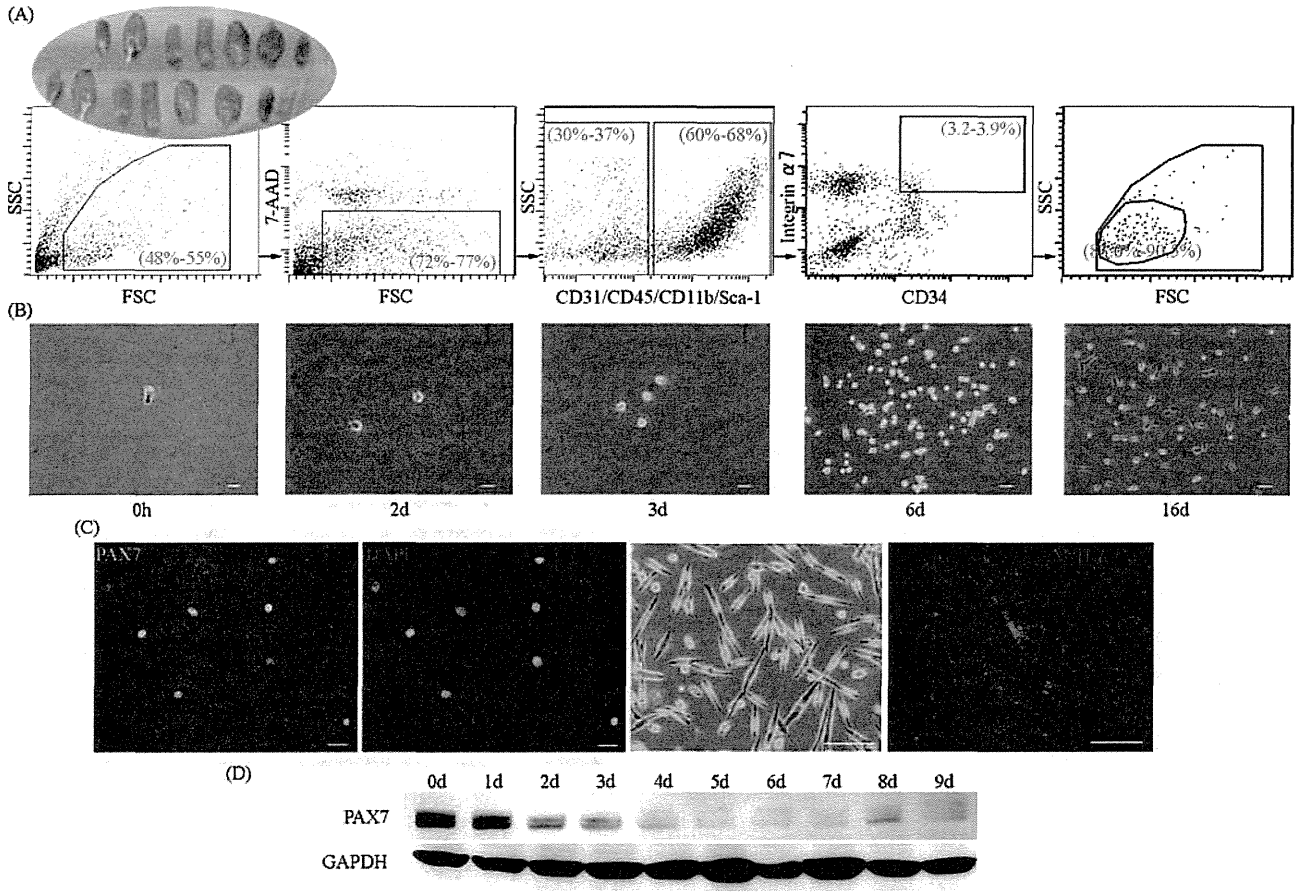

Figure 1. The isolation and characterization of the satellite cells. (**A**) A flow cytometer sorted the satellite cells from the hind-limb muscles after enzymatic dissociation (shown in circle on the left: upper muscles were isolated from a right leg and lower muscles were isolated from a left leg; from left to right: tibialis anterior, triceps surae, quadriceps, divided biceps femoris into two, gluteus maximus, and iliopsoas muscles) by gating for 7-AAD negative, then for CD31, CD45, CD11b, and Sca1 negative, and finally for integrin-α7 and CD34 positive. Numbers in the gates show percentage of the cells in each gate among total cells. (**B**) The light phase-contrast microscopy shows the morphology of the isolated satellite cells cultured in proliferation medium for the indicated time periods. Scale bars: 50 μm (left three panels) and 25 μm (right two panels). (**C**) The sorted cells were immunoreactive with satellite cell marker Pax7 and nucleus marker DAPI after 2 days in the proliferation medium (left two panels: Pax7 in green and DAPI in blue). After 3 days in the differentiation medium, some cells formed tube-like shapes (the third panel from the left) and some cells were immunoreactive with an immature myotube marker eMyHc (right panel: eMyHc in red and DAPI in blue). Scale bars: 20 μm (left two panels) and 50 μm (right two panels). (**D**) Western blot analysis shows the levels of PAX7 protein in the satellite cells after the induction of differentiation for the indicated time periods. The GAPDH protein is a loading control.

iliopsoas muscle) and sorted them according to the cell surface markers (Figure 1A). We characterized satellite cells as 7-AAD (a dead cell marker) negative, CD31 (an endothelial cell marker) negative, CD45 (a pan-hematopoietic cell marker) negative, CD11b (a myeloid cell marker) negative, Sca1 (a mesenchymal cell marker) negative, and integrin-α7 and CD34 positive (Figure 1A). We cultured the sorted cells in growth medium for several days and noted the proliferation of these cells, which suggested that these cells had the potential to re-enter the cell cycle (Figure 1B). After 2 days in the growth medium, the sorted cells were immunoreactive with satellite cell–specific transcriptional factor Pax7 and nucleus marker DAPI (Figure 1C, two panels in the left). To examine the potential of these cells to differentiate into myotubes, we cultured the cells in differentiation medium for 3 days (Figure 1C, two panels in the right). The cells fused and were immunoreactive with an immature myotube marker embryonic myosin heavy chain (eMyHc, Figure 1C, the right panel), suggesting that the cells differentiated into myotubes. The sorted cells were cultured in the differentiation medium, and the expression levels of Pax7 gradually decreased in a time-dependent manner after the induction of differentiation (Figure 1D). These data suggested that the sorted cells had the characteristics of satellite cells and the potential to differentiate into myotubes.

Effects of RJ/pRJ on the Satellite Cells of the Aged Mice In Vitro

To examine the effect of RJ/pRJ on the proliferation rate of the satellite cells of the aged mice in vitro, we isolated satellite cells from aged mice and stimulated them with RJ/pRJ for 24 hours (Figure 2A, left panel), 48 hours (Figure 2A, center panel), or 72 hours (Figure 2A, right

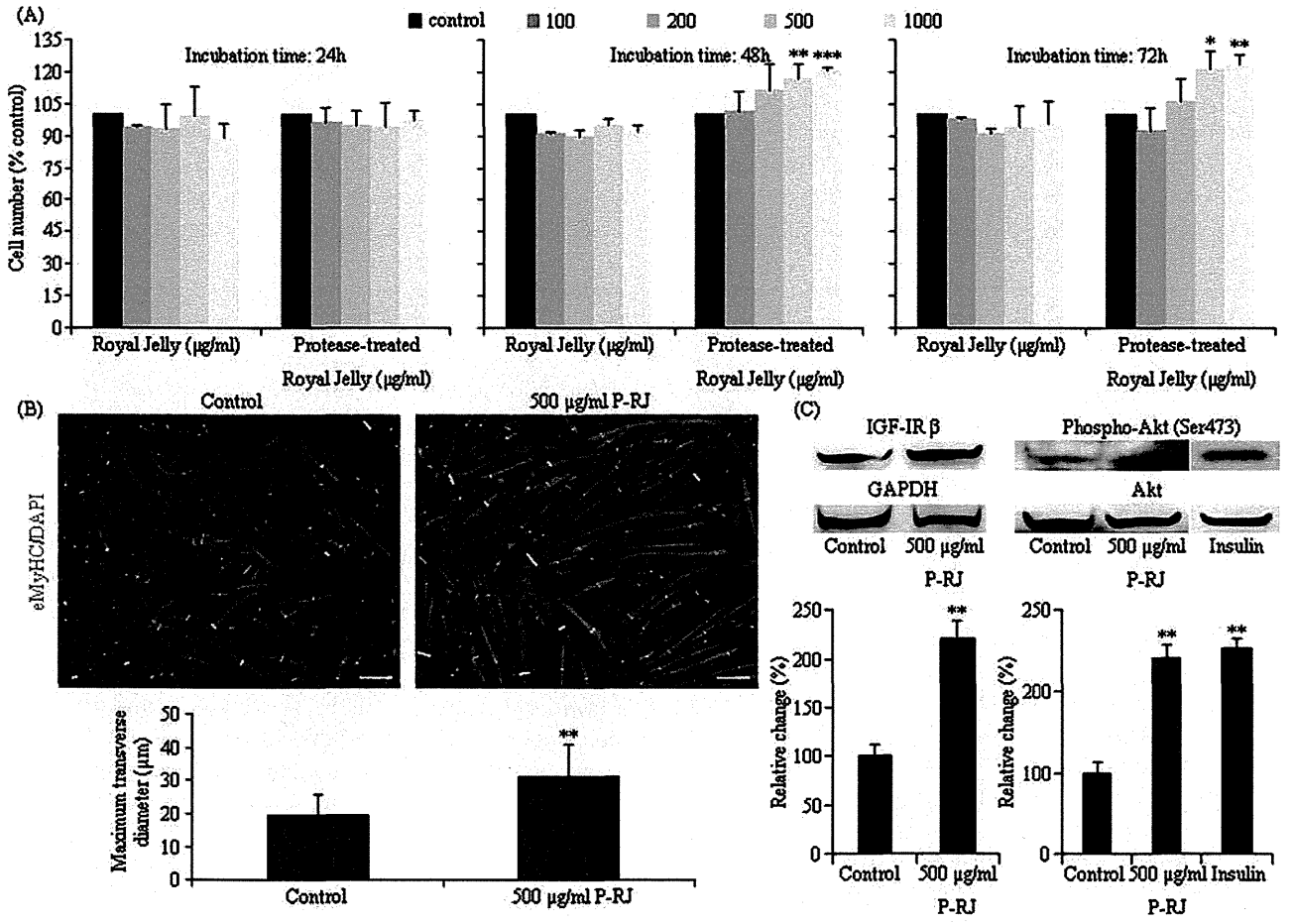

Figure 2. Effects of RJ/pRJ on the satellite cells of aged mice in vitro. (**A**) The satellite cells of the aged mice were treated with the indicated concentrations of RJ or pRJ for 24, 48, or 72 h, and the cell proliferation rate was measured at each time point. (**B**) The satellite cells of aged mice were cultured in differentiation medium with pRJ or without pRJ (control) for 5 days, then immunohistochemically stained for eMyHC in red and for DAPI in blue to evaluate their differentiation into myotubes. The maximum diameter of each myotube was marked with a green line (upper panels). We randomly selected 50 myotubes per field at ×400 magnification, measured the maximum diameter of each myotube for 10 randomly selected fields per sample, measured the diameter, and calculated for each group (lower panel). Scale bars: 100 μm. (**C**) The satellite cells of aged mice were pretreated with pRJ (500 μg/mL) for 48 h, then the Western blot analysis detected IGF-1 receptor (IGF-IR), GAPDH, activated form of Akt (phospho-Akt), and total Akt. Insulin (10 nM) was used as a positive control. The densitometry quantified the band intensities. The graphs show the IGF-IR band intensities normalized by the GAPDH band intensities, and phospho-Akt band intensities normalized by the Akt band intensities. This figure is the representative of three independent experiments. Columns are mean ± *SD*. $*p < .05$, $**p < .01$, and $***p < .0001$, compared with control.

panel) in growth medium. pRJ treatment at high concentrations (500 and 1000 μg/mL) for 48 and 72 hours increased the proliferation rate of the satellite cells compared with controls and RJ treatment (Figure 2A). Next, to examine the effect of RJ/pRJ on the differentiation of the satellite cells of the aged mice in vitro, we cultured the satellite cells in differentiation medium for 5 days and immunohistochemically stained them for eMyHC (Figure 2B). The pRJ-treated group had more eMyHc immunoreactive areas than did the controls (Figure 2B, upper panel). The mean maximum diameter of the myotubes was greater in the pRJ-treated group than in the controls (Figure 2, lower panel). These results suggested that pRJ promoted the differentiation of the satellite cells of the aged mice. We next examined an intracellular signaling pathway of IGF-1 by Western blot analysis. pRJ treatment increased the intensity of the band of IGF-1R compared with controls (Figure 2C). One of the downstream signaling pathways of IGF-1R is Akt, and pRJ treatment increased the intensity of the band of phosphorylated Akt, which is an activated form of Akt, compared with controls (Figure 2C). Similar to pRJ, the increased activation of Akt was also observed in satellite cells treated with 10 nM insulin (Figure 2C). These results suggested that pRJ increased the proliferation rate, promoted differentiation, and activated the Akt-signaling pathway in the satellite cells from the aged mice compared with the controls in vitro.

RJ-/pRJ-Treated Mice Had Greater Numbers of Satellite Cells, Muscle Weight, and Grip Strength Than Did Controls

To examine the effects of RJ/pRJ treatment on aged mice in vivo, we divided 21-month-old mice into five groups and treated them with five kinds of diets for 3 months, respectively: normal diet (controls), diet mixed with 1% weight RJ (1% RJ), diet with 5% weight RJ (5% RJ), diet with 1% weight pRJ (1% pRJ), and diet with 5% pRJ (5% pRJ). Three mice in the controls, one mouse in the 1% RJ group, and one mouse in the 1% pRJ group died of natural causes during the treatment period. These mice were excluded from the analysis. During the intervention period, the body weight increased similarly in RJ/pRJ-treated groups and control groups (Figure 3A) (p value $> .73$; effect size ≤ 0.01). The amount of daily diet intake was not different between the groups (Figure 3B). Comparison of the hind-limb muscle weight per body weight between 2-, 8-, and 24-month-old mice showed progressive loss of muscle weight with aging, suggesting the progression of sarcopenia with aging (Figure 3C). The combined weights of the hind-limb muscles of one leg, named one-legged muscle, per body weight in 5% RJ, 1% pRJ, and 5% pRJ groups were greater than those of controls (Figure 3D). The selected muscles included the TA, triceps surae, quadriceps, biceps femoris, gluteus maximus, and iliopsoas muscles. To examine the effect of PJ/pRJ on the numbers of satellite cells in vivo, we counted the cells. The numbers of satellite cells in the hind-limb muscles in the 5% RJ- and 5% pRJ-treated groups were significantly greater than those of the controls (Figure 3E), whereas the numbers of the satellite cells per muscle weight were not different among the groups (per gram; Figure 3F). These results suggested that PJ/pRJ treatment increased the total numbers of satellite cells.

To examine the effect of pRJ on the muscle strength, we performed the wire hang test and measured the maximum duration that the mice could hang on the inverted wire mesh. Consistent with the effect of RJ/pRJ on the muscle mass, the 5% RJ- and 5% pRJ-treated groups hung for longer duration than did the controls, suggesting that RJ/pRJ improved the grip strength of the skeletal muscles (Figure 3G). To examine the effect of RJ/pRJ on muscle fatigue, we measured how many times the mice could hang from the wire mesh. The 5% RJ- and 5% pRJ-treated groups could hang more times than the controls, suggesting that RJ/pRJ improved the fatigue of the skeletal muscles (Figure 3H). Furthermore, within the controls, comparison of the before and after treatment period showed decreased hanging duration and times after the treatment period than before, suggesting the progression of age-related atrophy in muscle function. In contrast, no significant changes were observed within the RJ/pRJ groups between before and after the treatment period. These data suggested that RJ/pRJ treatment prevented the progression of atrophy in muscle weight and function in the aged mice.

RJ/pRJ Treatment Accelerated the Regeneration of Injured Skeletal Muscles

We next examined the effect of RJ/pRJ treatment on the regenerating capacity of the skeletal muscles in aged mice in vivo by injuring the TA muscles with cardiotoxin injection and observing their regeneration. We isolated the muscles 5 days after the cardiotoxin injection and subjected them to staining. Hematoxylin and eosin staining showed greater amounts of muscle fibers in the RJ/pRJ groups than in the controls (Figure 4A, upper panels). To confirm the regenerating capacity of the skeletal muscles, we immunohistochemically stained the muscles for eMyHc, which is a marker of immature myotubes including regenerating muscles but not of mature muscles (Figure 4A, middle line panels). Quantification of the eMyHc immunoreactive area showed greater immunoreactive areas in the RJ/pRJ groups than in the controls (Figure 4B). These results suggested that RJ/pRJ treatment accelerated the regeneration of the injured skeletal muscles.

RJ/pRJ Treatment Increased Serum IGF-1 Levels

Because RJ has been suggested to have an anti-inflammatory effect, we examined the effect of RJ/pRJ treatment on serum proinflammatory mediator levels in the aged mice.

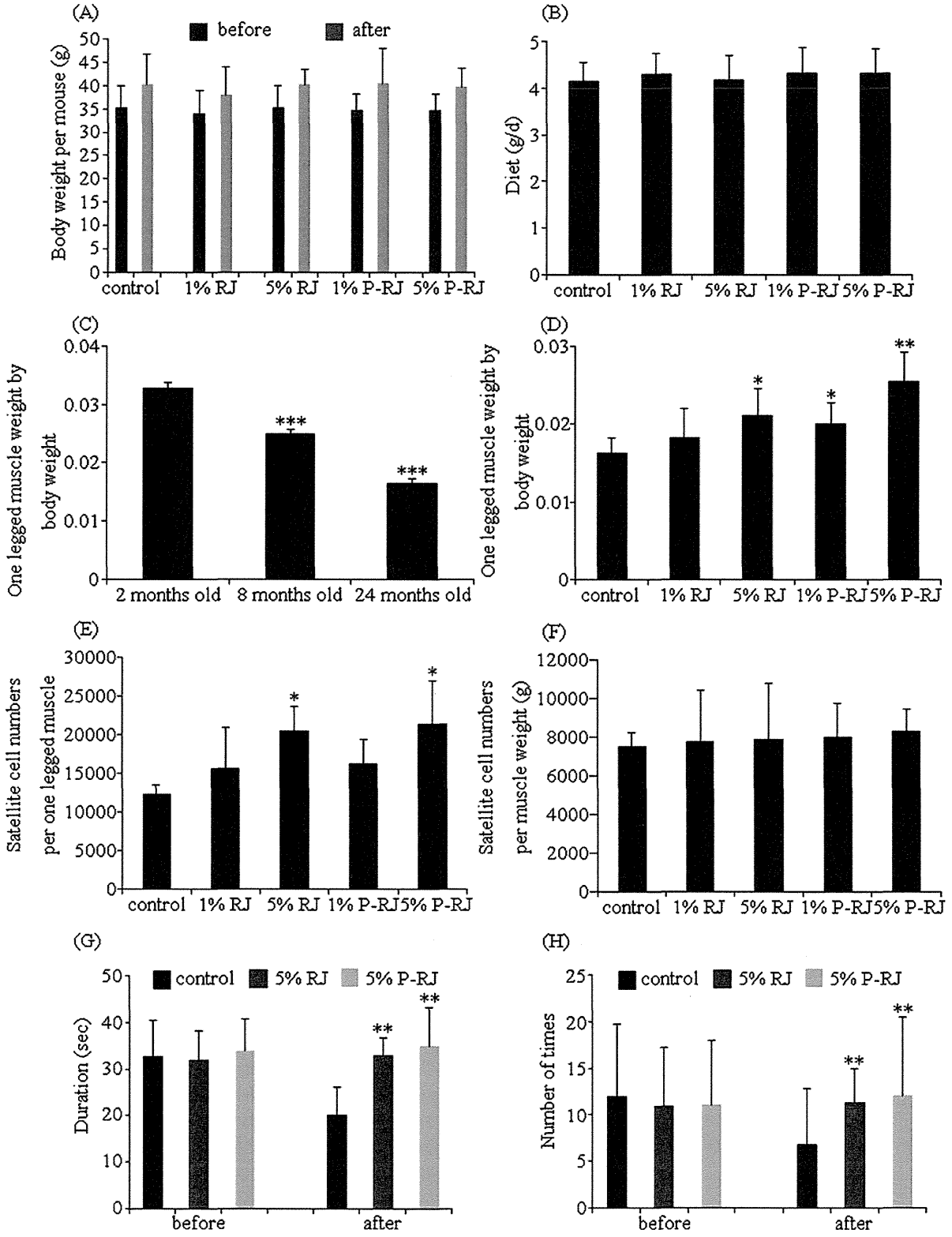

Figure 3. Effects of RJ/pRJ treatment on aged mice in vivo. Twenty-one-month-old mice were treated with a diet mixed with 1% weight RJ (1% RJ), diet with 5% weight RJ (5% RJ), diet with 1% weight pRJ (1% pRJ), or diet with 5% pRJ (5% pRJ) for following 3 months. (**A**) Control, RJ, or pRJ treatment did not show changed body weight. (**B**) RJ or pRJ did not change the amount of the daily diet intake. (**C**) The progressive loss of muscle weight with aging. (**D**) RJ- and pRJ-treated groups had greater hind-limb muscle weights per body weight than did controls. (**E**) RJ- and pRJ-treated groups had greater numbers of satellite cells in the hind-limb muscles than did controls. (**F**) RJ or pRJ treatment did not change the numbers of satellite cells per muscle weight (g). (**G**) Five% RJ- and pRJ-treated mice hung for longer durations than did controls. (**H**) Five% RJ- and pRJ-treated mice hung more times than did controls. Columns are mean ± *SD*, $n \geq 5$ in each group. $^{*}p < .05$, $^{**}p < .01$, and $^{***}p \leq .0001$ compared with control.

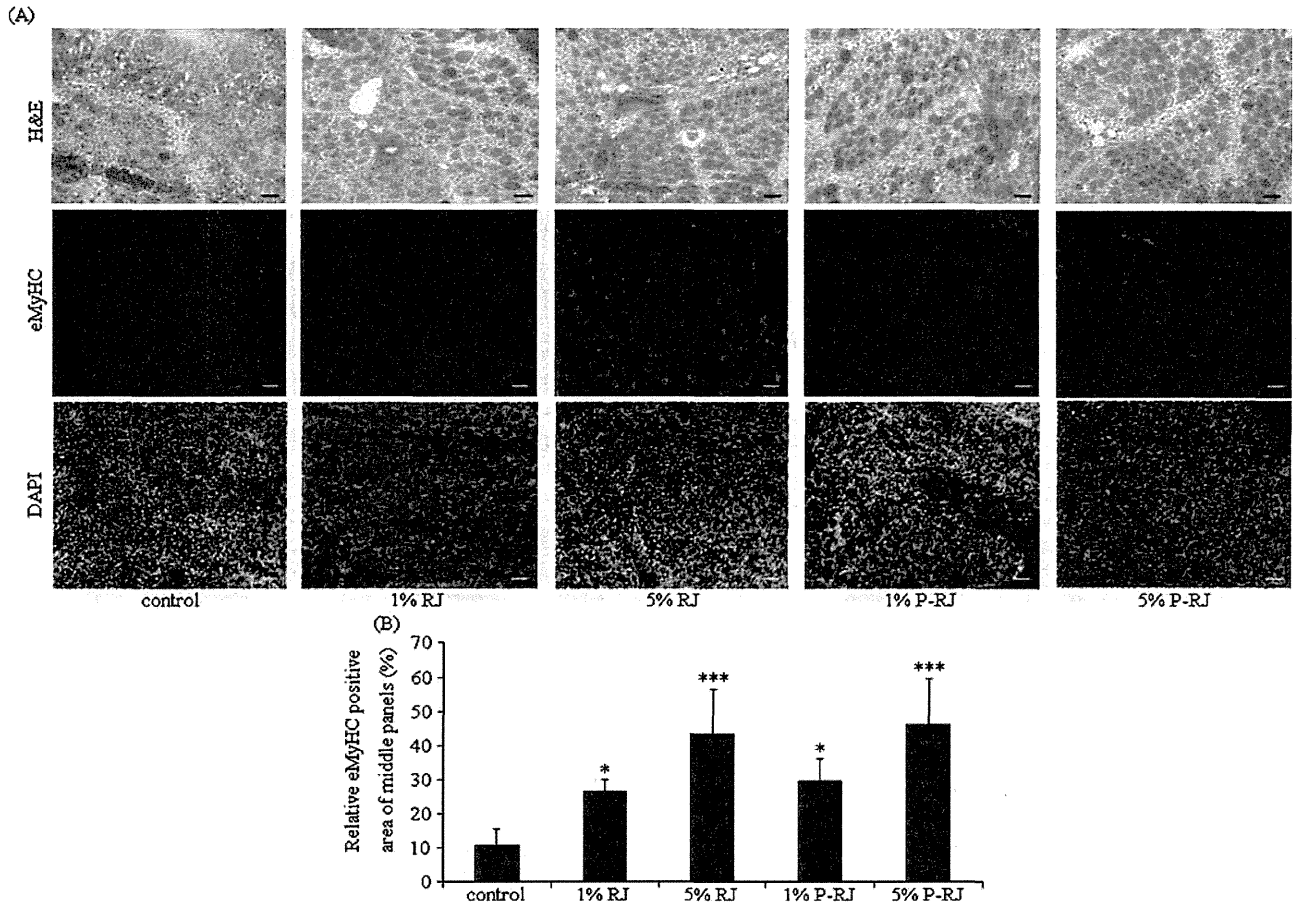

Figure 4. RJ/pRJ treatment accelerated the regeneration of the injured skeletal muscles in aged mice. After 3 months of RJ/pRJ treatment, we injected cardiotoxin into the tibialis anterior muscles of the aged mice to injure the muscles and isolated them 5 days later. (**A**) Hematoxylin and eosin staining (top panels) and immunohistochemical staining for eMyHC (middle panels) or DAPI (bottom panels) of the injured tibialis anterior muscles. Upper lines, scale bar, 50 μm; middle and lower lines, scale bar, 100 μm. (**B**) The graph shows the data calculated from quantification of the percentage of eMyHc-immunoreactive area per field for each group (10 randomly selected fields at ×200 magnification per sample were quantified). Columns are mean ± *SD*, $n \geq 3$ in each group. $^{*}p < .05$, and $^{***}p < .0001$ compared with controls.

We chose IL-1α, IL-1β, IL-6, and tumor necrosis factor-α as proinflammatory mediators, as previously shown (31,32), and measured their levels in serum. The levels of these mediators were not significantly different between RJ-/pRJ-treated groups and controls, but the serum IL-1α concentration tended to be lower in the RJ/pRJ groups than in the controls (Figure 5A). Because IGF-1 plays a central role in stimulating satellite cells, we measured the serum levels of IGF-1. The serum levels of IGF-1 were greater in the 5% RJ- and pRJ-treated groups than in the controls (Figure 5B).

Discussion

In this study, using aged mice, we showed that RJ/pRJ treatment increased the number of satellite cells, the skeletal muscle weight, grip strength, regenerating capacity of injured skeletal muscles, and the serum IGF-1 levels compared with controls in vivo. In vitro, compared with controls, pRJ treatment increased the cell proliferation rate, promoted differentiation, and activated the Akt-signaling pathway in the satellite cells of the aged mice.

RJ/pRJ treatment increased the number of satellite cells of the aged mice, promoted their differentiation compared with controls, which could be the mechanisms by which the skeletal muscle weight and grip strength were increased, and accelerated the regeneration of injured skeletal muscles in aged mice compared with controls. Because these effects antagonized the loss of muscle mass and strength, the results suggested that RJ/pRJ treatment might improve sarcopenia in aged mice. The RJ-/pRJ-treated groups hung for longer durations than did the controls, but when we compared between before and after the treatment period within the same groups, the hanging duration did not change in the RJ-/pRJ-treated groups, whereas the hanging duration decreased after the same period in controls, suggesting that RJ/pRJ treatment might not improve but rather attenuated the progression of the decrease in grip strength. Therefore, the effects of RJ/pRJ on skeletal muscles might be

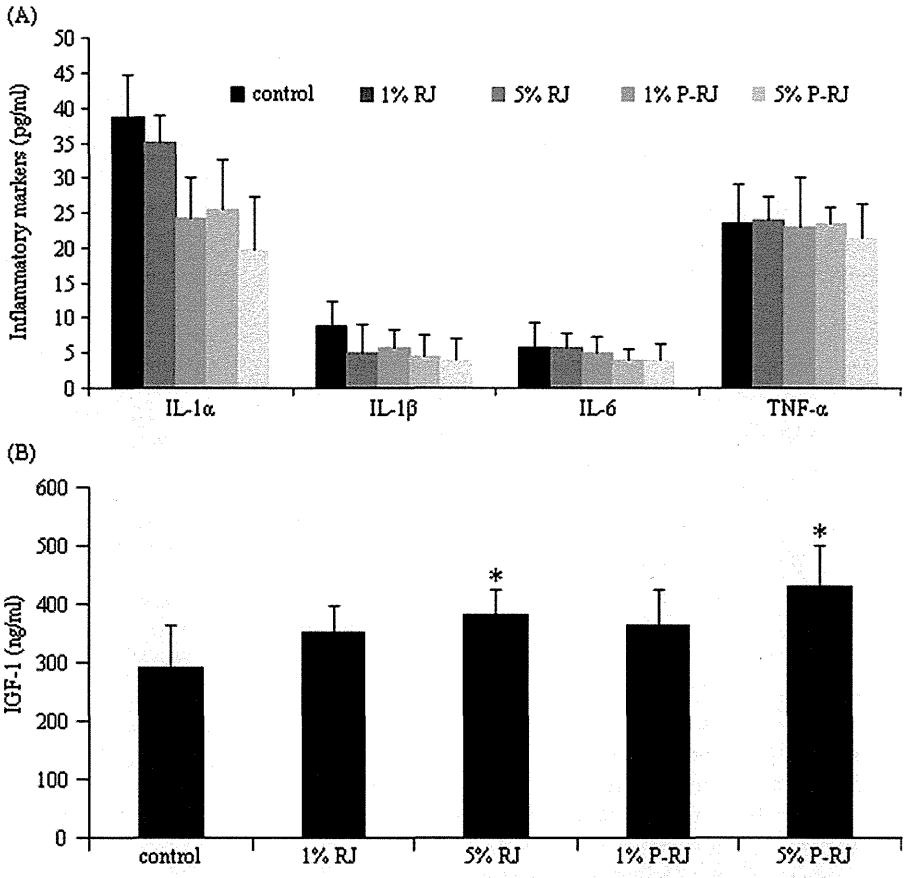

Figure 5. RJ/pRJ treatment increased the serum IGF-1 levels but did not affect the serum proinflammatory mediator levels. ELISA determined serum levels of proinflammatory mediators and IGF-1 in aged mice treated with RJ/pRJ for 3 months. (**A**) RJ/pRJ treatment did not change the serum levels of the proinflammatory mediators. (**B**) Five% RJ and 5% pRJ treatment significantly increased the serum IGF-1 levels. Columns are mean ± *SD*, $n = 5$ in each group. *$p < .05$ compared with controls.

attenuating the atrophy rather than improving the muscle mass and strength in aged mice.

pRJ increased the number of satellite cells of the aged mice in vivo and in vitro, whereas RJ increased the number of the satellite cells in vivo but not in vitro. The presence of protease treatment in pRJ and its absence in RJ might explain this discrepancy. Protease is present in vivo, which indicates that all the RJ is treated with protease after their intake in vivo, whereas protease is not present in vitro.

Because IGF-1 has favorable effects on satellite cells, the skeletal muscles, and sarcopenia, the increased serum levels of IGF-1 after RJ/pRJ treatment might be one of the mechanisms of the effects of RJ/pRJ treatment. However, the increases in the levels of IGF-1 after RJ/pRJ treatment were moderate. Therefore, RJ/pRJ treatment may have other mechanisms besides increasing IGF-1. Previous studies indicated that nutrition plays a central role in the regulation of the IGF-1 levels (33). The serum IGF-1 levels decline in an age-dependent manner and are a reliable index of protein-energy malnutrition in elderly patients (34–36). Increased serum levels of IGF-1 after RJ/pRJ treatment may suggest that RJ/pRJ treatment improved the malnutrition in the aged animals. Many nutritional components in RJ/pRJ such as vitamins, minerals (Table 1), and amino acids might have contributed to preventing sarcopenia. Because this is a single study, we could not evaluate the contribution of each component to the prevention of sarcopenia. However, the results suggested that whole RJ/pRJ improved sarcopenia in aged mice.

Akt-signaling pathway plays a central role in muscle protein synthesis and in inhibiting muscle proteolysis. Akt activation prevents muscle atrophy including sarcopenia (37). Moreover, the activation of Akt in myoblasts increased their cell proliferation rate and rescued them from cell death (22). In vitro, pRJ activated the Akt-signaling pathway in satellite cells of the aged mice. Because pRJ contains a wide variety of components (9), it is not clear which component(s) activated Akt. However, the activation of Akt, possibly by IGF-1, suggests that one of the mechanisms of the effects of RJ/pRJ was via Akt. Furthermore, because RJ and pRJ are natural products, some natural factors such as seasonal or environmental factors may affect the percentage or quality of ingredients in RJ/pRJ. Further studies are required to identify the mechanisms of action of RJ/pRJ.

Some studies reported that IGF-1 deficiency extended life spans in mammals (38,39). Because we did not assess life

spans in this study, the effect of increased levels of IGF-1 by RJ/pRJ treatment on life span was not clear. However, previous studies reported that RJ/pRJ extended the life span in mice and *Caenorhabditis elegans* (10,11). Further studies are required to evaluate the effects and mechanisms of RJ/pRJ on life span.

Dietary supplementation with 1%–5% RJ/pRJ would be too great in an amount and would not be feasible for humans. Generally, dietary supplementation intake in animals cannot be directly converted into human dietary intake. Thus, we did a pilot study to examine the effect of RJ on muscle strength and physical performance in free-living elderly patients (Identifier: UMIN000004057, Trial Registration: http://www.umin.ac.jp/ctr/index.htm). We found that the intake of RJ (low dose: 1.2 g/day; high dose: 4.8 g/day) for 3 months improved muscle strength and physical performance in the elderly patients. Based on this pilot study, we are performing a randomized, double-blinded, placebo-controlled trial to confirm the effects of RJ on muscle strength and physical performance of the elderly patients (Identifier: UMIN000009648, Trial Registration: http://www.umin.ac.jp/ctr/index.htm).

In conclusion, in vivo, RJ/pRJ treatment increased the muscle weight, grip strength, regenerating capacity of injured muscles, and serum IGF-1 levels compared with controls in aged mice. In vitro, pRJ increased the cell proliferation rate, promoted the cell differentiation, and activated Akt-signaling pathway compared with controls in isolated satellite cells from aged mice. These findings suggest that RJ/pRJ treatment may have a beneficial effect on the prevention of age-related sarcopenia through increasing the systemic IGF-1 levels and activating Akt-signaling pathways in satellite cells.

FUNDING

This research was supported by Yamada Research Grant.

CONFLICT OF INTERESTS

All the authors have no conflicts of interest to disclose.

REFERENCES

1. Nations United. *Department of Economic and Social Affairs Population Division: World Population Ageing 2009*. New York: United Nations; 2009:11.
2. Altun M, Grönholdt-Klein M, Wang L, Ulfhake B. Cellular degradation machineries in age-related loss of muscle mass (Sarcopenia). In: Nagata T, ed. *Senescence*. San Francisco, CA: Academia.edu; 2012:269–286.
3. Hawke TJ, Garry DJ. Myogenic satellite cells: physiology to molecular biology. *J Appl Physiol*. 2001;91:534–551.
4. Clemmons DR. Role of IGF-I in skeletal muscle mass maintenance. *Trends Endocrinol Metab*. 2009;20:349–356.
5. Welle S. Cellular and molecular basis of age-related sarcopenia. *Can J Appl Physiol*. 2002;27:19–41.
6. Sacco A, Doyonnas R, Kraft P, Vitorovic S, Blau HM. Self-renewal and expansion of single transplanted muscle stem cells. *Nature*. 2008;456:502–506.
7. Giovannini S, Marzetti E, Borst SE, Leeuwenburgh C. Modulation of GH/IGF-1 axis: potential strategies to counteract sarcopenia in older adults. *Mech Ageing Dev*. 2008;129:593–601.
8. Viuda-Martos M, Ruiz-Navajas Y, Fernández-López J, Pérez-Alvarez JA. Functional properties of honey, propolis, and royal jelly. *J Food Sci*. 2008;73:R117–R124.
9. Sabatini AG, Marcazzan GL, Caboni MF, Bogdanov S, Almeida-Muradian LBd. Quality and standardisation of Royal Jelly. *J ApiProduct ApiMedical Sci*. 2009;1:1–6.
10. Inoue S, Koya-Miyata S, Ushio S, Iwaki K, Ikeda M, Kurimoto M. Royal Jelly prolongs the life span of C3H/HeJ mice: correlation with reduced DNA damage. *Exp Gerontol*. 2003;38:965–969.
11. Honda Y, Fujita Y, Maruyama H, et al. Lifespan-extending effects of royal jelly and its related substances on the nematode Caenorhabditis elegans. *PLoS One*. 2011;6:e23527.
12. Kamakura M, Mitani N, Fukuda T, Fukushima M. Antifatigue effect of fresh royal jelly in mice. *J Nutr Sci Vitaminol (Tokyo)*. 2001;47:394–401.
13. Matsui T, Yukiyoshi A, Doi S, Sugimoto H, Yamada H, Matsumoto K. Gastrointestinal enzyme production of bioactive peptides from royal jelly protein and their antihypertensive ability in SHR. *J Nutr Biochem*. 2002;13:80–86.
14. Vittek J. Effect of royal jelly on serum lipids in experimental animals and humans with atherosclerosis. *Experientia*. 1995;51:927–935.
15. Liu JR, Yang YC, Shi LS, Peng CC. Antioxidant properties of royal jelly associated with larval age and time of harvest. *J Agric Food Chem*. 2008;56:11447–11452.
16. Kohno K, Okamoto I, Sano O, et al. Royal jelly inhibits the production of proinflammatory cytokines by activated macrophages. *Biosci Biotechnol Biochem*. 2004;68:138–145.
17. Macaluso A, De Vito G. Muscle strength, power and adaptations to resistance training in older people. *Eur J Appl Physiol*. 2004;91:450–472.
18. Strasser EM, Wessner B, Roth E. Cellular regulation of anabolism and catabolism in skeletal muscle during immobilisation, aging and critical illness. *Wien Klin Wochenschr*. 2007;119:337–348.
19. Schaap LA, Pluijm SM, Deeg DJ, Visser M. Inflammatory markers and loss of muscle mass (sarcopenia) and strength. *Am J Med*. 2006;119:526.e9–526.17.
20. Meng SJ, Yu LJ. Oxidative stress, molecular inflammation and sarcopenia. *Int J Mol Sci*. 2010;11:1509–1526.
21. Sriram S, Subramanian S, Sathiakumar D, et al. Modulation of reactive oxygen species in skeletal muscle by myostatin is mediated through NF-κB. *Aging Cell*. 2011;10:931–948.
22. Okazaki T, Ebihara S, Asada M, et al. Macrophage colony-stimulating factor improves cardiac function after ischemic injury by inducing vascular endothelial growth factor production and survival of cardiomyocytes. *Am J Pathol*. 2007;171:1093–1103.
23. Yahiaoui L, Gvozdic D, Danialou G, Mack M, Petrof BJ. CC family chemokines directly regulate myoblast responses to skeletal muscle injury. *J Physiol*. 2008;586:3991–4004.
24. Okazaki T, Ebihara S, Asada M, Yamanda S, Niu K, Arai H. Erythropoietin promotes the growth of tumors lacking its receptor and decreases survival of tumor-bearing mice by enhancing angiogenesis. *Neoplasia*. 2008;10:932–939.
25. Nakajima R, Takao K, Huang SM, et al. Comprehensive behavioral phenotyping of calpastatin-knockout mice. *Mol Brain*. 2008;7:1–15.
26. Uezumi A, Fukada S, Yamamoto N, Takeda S, Tsuchida K. Mesenchymal progenitors distinct from satellite cells contribute to ectopic fat cell formation in skeletal muscle. *Nat Cell Biol*. 2010;12:143–152.
27. Niu K, Asada M, Okazaki T, et al. Adiponectin pathway attenuates malignant mesothelioma cell growth. *Am J Respir Cell Mol Biol*. 2012;46:515–523.
28. Fukada S, Yamaguchi M, Kokubo H, et al. Hesr1 and Hesr3 are essential to generate undifferentiated quiescent satellite cells and to maintain satellite cell numbers. *Development*. 2011;138:4609–4619.
29. Asada M, Ebihara S, Yamanda S, et al. Depletion of serotonin and selective inhibition of 2B receptor suppressed tumor angiogenesis by

inhibiting endothelial nitric oxide synthase and extracellular signal-regulated kinase ½ phosphorylation. *Neoplasia*. 2009;11:408–417.
30. Yamanda S, Ebihara S, Asada M, et al. Role of ephrinB2 in non-productive angiogenesis induced by Delta-like 4 blockade. *Blood*. 2009;113:3631–3639.
31. Okazaki T, Sakon S, Sasazuki T, et al. Phosphorylation of serine 276 is essential for p65 NF-kappaB subunit-dependent cellular responses. *Biochem Biophys Res Commun*. 2003;300:807–812.
32. Okazaki T, Ni A, Baluk P, et al. Capillary defects and exaggerated inflammatory response in the airways of EphA2-deficient mice. *Am J Pathol*. 2009;174:2388–2399.
33. Chevenne D, Porquet D. Growth hormone (GH) and insulin-like growth factor 1 (IGF-1) in nutritional status. *Ann Biol Clin (Paris)*. 1995;53:527–538.
34. Campillo B, Paillaud E, Bories PN, Noel M, Porquet D, Le Parco JC. Serum levels of insulin-like growth factor-1 in the three months following surgery for a hip fracture in elderly: relationship with nutritional status and inflammatory reaction. *Clin Nutr*. 2000;19:349–354.
35. Ponzer S, Tidermark J, Brismar K, Söderqvist A, Cederholm T. Nutritional status, insulin-like growth factor-1 and quality of life in elderly women with hip fractures. *Clin Nutr*. 1999;18:241–246.
36. McWhirter JP, Ryan MF, Pennington CR. An evaluation of insulin-like growth factor-1 as an indicator of nutritional status. *Clin Nutr*. 1995;14:74–80.
37. Kandarian SC, Jackman RW. Intracellular signaling during skeletal muscle atrophy. *Muscle Nerve*. 2006;33:155–165.
38. Carter CS, Ramsey MM, Ingram RL, et al. Models of growth hormone and IGF-1 deficiency: applications to studies of aging processes and life-span determination. *J Gerontol A Biol Sci Med Sci*. 2002;57:B177–B188.
39. Chiba T, Yamaza H, Shimokawa I. Role of insulin and growth hormone/insulin-like growth factor-I signaling in lifespan extension: rodent longevity models for studying aging and calorie restriction. *Curr Genomics*. 2007;8:423–428.

PLOS ONE

Waist to Height Ratio Is an Independent Predictor for the Incidence of Chronic Kidney Disease

Keiichi Odagiri[1]*, Isagi Mizuta[2], Makoto Yamamoto[2], Yosuke Miyazaki[3], Hiroshi Watanabe[1], Akihiko Uehara[2]

1 Department of Clinical Pharmacology and Therapeutics, Hamamatsu University School of Medicine, Higashi-ku, Hamamatsu, Japan, **2** Yamaha Health Care Center, Naka-ku, Hamamatsu, Japan, **3** Department of Mental Health, Institute of Industrial Ecological Sciences, School of Medicine, University of Occupational and Environmental Health, Yahatanishi-ku, Kitakyushu, Japan

Abstract

Objective: Obesity is a risk factor for chronic kidney disease (CKD) and cardiovascular disease. The association between waist to height ratio (WheiR) and CKD is unclear. This study evaluated the association between WheiR and CKD.

Design and Methods: In this longitudinal cohort study, 4841 Japanese workers (3686 males, 1155 females) 18 to 67 years of age in 2008 were followed up until 2011. CKD was defined as an estimated glomerular filtration rate of <60 mL/min/1.73 m^2 (by the Modification of Diet in Renal Disease equation for Japanese) or dipstick proteinuria (≥1+). Cox proportional hazards models were used to examine the relationship between WheiR and development of CKD.

Results: A total of 384 (7.9%) participants (300 men and 84 women) were found to have new CKD. The incidence of CKD was 13.7, 24.2, 37.9 and 43.7 per 1000 person-years of follow-up in the lowest, second, third and highest quartiles of WheiR, respectively. After adjustment for potential confounders, the adjusted hazard ratios (95% confidence interval) for CKD were 1.00 (reference), 1.23 (0.85, 1.78), 1.59 (1.11, 2.26) and 1.62 (1.13, 2.32) through the quartiles of WheiR, respectively. WheiR had a significant predictive value for the incidence of both proteinuria and low estimated glomerular filtration rate. After subdivision according to gender, the relationship between WheiR and the incidence of CKD was statistically significant in the unadjusted model. However, after adjusting for potential confounders, WheiR was significantly associated with the incidence of CKD in females, whereas it was not significant in males.

Conclusions: WheiR, which is commonly used as an index of central obesity, is associated with CKD. There was a significant gender difference in the relationship between CKD and WheiR.

Citation: Odagiri K, Mizuta I, Yamamoto M, Miyazaki Y, Watanabe H, et al. (2014) Waist to Height Ratio Is an Independent Predictor for the Incidence of Chronic Kidney Disease. PLoS ONE 9(2): e88873. doi:10.1371/journal.pone.0088873

Editor: Giuseppe Danilo Norata, University of Milan, Italy

Received September 2, 2013; **Accepted** January 14, 2014; **Published** February 12, 2014

Funding: Hiroshi Watanabe received research funding from the Ministry of Health, Labour and Welfare of Japan, Teika Seiyaku, Takeda Pharmaceuticals, Mochida, Pfizer, Astellas Pharmaceuticals, and Daiichi Sankyo. The commercial funding is not specifically related to the study, and there are no other current external funding sources for this study. The funders had no role in study design, data collection and analysis, decision to publish, or preparation of the manuscript.

Competing Interests: Hiroshi Watanabe has received lecture fees from Pfizer, Acterion, Novartis, Daiichi Sankyo, GlaxoSmithKline and Nippon Shinyaku. This does not alter the authors' adherence to all the PLOS ONE policies on sharing data and materials.

* E-mail: kodagiri@hama-med.ac.jp

Introduction

Chronic kidney disease (CKD) is a relatively common disorder. Patients with CKD have an increased risk of end-stage renal disease. Furthermore, CKD is also related to both a higher prevalence of cardiovascular disease and premature death [1,2]. The estimated proportion of patients with CKD in the general population is approximately 10% in the United States, 7% in the United Kingdom, 9−10% in Asian countries and 19% in Japan [3–7]. The prevalence of CKD has been increasing significantly with time [8,9]. Therefore, screening, diagnosis and treatment of CKD are important issues in preventing disease onset and progression [10,11].

A recent study reported that obesity is a primary risk factor for cardiovascular disease, diabetes mellitus, hypertension and metabolic syndrome, and that these risk factors are associated with CKD [12]. Many authors consider that abdominal obesity is superior to body mass index (BMI) in predicting cardiometabolic risk, and visceral fat is known to have high metabolic and inflammatory activity in comparison to subcutaneous fat [13–17]. Waist to height ratio (WheiR) is recognized as an effective index for identifying central obesity, which relates to cardiometabolic risk factors [18]. One meta-analysis has demonstrated that WheiR is statistically superior to both waist circumference (WC) and BMI in the evaluation of cardiometabolic risk [19]. However, few studies have demonstrated an association between WheiR and CKD. Thus, we hypothesized that WheiR was associated with the incidence of CKD. We tested this hypothesis by investigating the 3-year incidence of CKD in Japanese workers.

Materials and Methods

Ethics Statement

The Institutional Review Board waived the need for informed consent from the participants because this research was a

retrospectively observational analysis, and the identifying information was not included in the collected data. The ethics committee of Yamaha Health Insurance Society approved this study.

Study Design and Participants

We designed a retrospective longitudinal cohort study to investigate the relation between WheiR and the incidence of newly diagnosed CKD in Japanese employees at general health checkups at the Yamaha Health Care Center, Hamamatsu, Japan. Most of the participants were employees of manufacturing companies in Hamamatsu, Japan. The Industrial Safety and Health Law in Japan requires employers to conduct annual health examinations of all employees. Our study utilized routinely collected data from these checkups. Because many participants were expected to have repeated examinations, we took advantage of this opportunity to conduct a follow-up study on CKD.

A total of 7025 participants (5337 men and 1688 women) who underwent general health checkup between January 2008 and December 2008 were enrolled in the study. Participants' ages ranged from 18 to 67 years (mean 41.7±11.1 years). After enrollment, the participants were followed up by general health checkups every year. We excluded 2184 participants who were already diagnosed with CKD (n = 545), lacked some laboratory data (n = 194) and had missing data for health behaviors (n = 3) at baseline. In addition, we excluded the participants who were not followed up in 2009 (n = 1442). Overall, the current analysis comprised 4841 participants (3686 men and 1155 women) with complete data on all the health behaviors and general health checkups. Among those participants, 673 were lost to follow up. However, we had no information on the causes of losing to follow up. The mean follow-up period was 2.7±0.7 years (range, 0.2−3.9), 12,926 person-years.

Data Collection and Measurements

Measurements. After an overnight fast, blood and urine samples were obtained to measure blood levels of routine medical checkup tests: The complete blood count was measured automatically in a Sysmex XE 2100 equipment (Roche Diagnostics, Kobe, Japan). Fasting plasma glucose (FPG), triglycerides (TG), creatinine (Crt) and low-density lipoprotein (LDL) cholesterol were measured enzymatically. High-density lipoprotein (HDL) cholesterol was measured using the precipitation method. Hemoglobin A1c (HbA1c) was measured using the latex agglutination method. Uric acid (UA) was measured using uricase/POD method, Liver function tests including γ-glutamyltransferase (GGT), aspartate aminotransferase (AST), alanine aminotransferase (ALT) were measured using LDH-UV method. Simple qualitative urinalyses were performed with a dipstick on flesh, mid-stream urine collection in the morning, as a single control test. Chemical measurements were all performed at a local laboratory (Medic, Hamamatsu, Japan). Systolic blood pressure (SBP) and diastolic blood pressure (DBP) were measured with the participants in a sitting position. Height and body weight were measured with the participants wearing lightweight clothing. WC was measured at navel level in a standing position with light expiration.

Questionnaire interview. Participants were all required to fill out a self-administered standardized questionnaire of "Specific Health Checkups" in Japan, which included information about lifestyle factors and medical history, including smoking status (never, former or current smoker), alcohol drinking behavior (non/rare, sometimes, everyday), regular exercise habit (exercising at least 2 days/week, at least 30 minutes) and antihypertensive, antidiabetic, antidyslipidemic and antihyperuricemic medications. Three health behaviors − smoking status, alcohol intake and regular exercise − were selected as study variables from self-administered questionnaires.

Definitions

BMI was calculated as weight in kilograms divided by the square of height in meters. Estimated glomerular filtration rate (eGFR) was calculated as eGFR (mL/min/1.73 m^2) = 194×Crt $^{-1.094}$ × age $^{-0.287}$ in men, and 194× creatinine $^{-1.094}$ × age $^{-0.287}$×0.739 in women according to the criteria of the Japanese Society of Nephrology [20]. WheiR was calculated by dividing the WC by body height. Low eGFR was defined as eGFR < 60 mL/min/1.73 m^2. Proteinuria was defined as dipstick proteinuria (≥1+). CKD was diagnosed on the basis of low eGFR and/or proteinuria which were present in single test.

Follow-up and End Points

Participants were followed from the starting point until December 31, 2011. The primary end point of this analysis was an incidence of new CKD. Study participation was considered to be complete if the participant had an occurrence of the primary end point, was unable to be followed further because of loss of follow-up, or had been followed through at least to December 31, 2011. The exposure time was calculated as the time between the first visit to our institution and the point of either incidence of new CKD or the date of the last study visit if that came first.

Statistical Analysis

All the data were expressed as the mean ± standard deviation (SD) (parametrically distributed values) or median (interquartile range) (non-parametrically distributed values) of the indicated numbers. We divided the study population into gender-adjusted quartiles of the distribution of WheiR. Differences among the quartiles of WheiR were examined by one-way analyses of variance (ANOVA) (parametrically distributed values) or Kruskal-Wallis test (non-parametrically distributed values). The polynomial contrast test and Kendall tau rank correlation coefficient (Kendall's tau-b) were used for trend analysis of numerical and categorical variables. Categorical variables were compared among the quartiles of WheiR by the chi-square test. Cox proportional-hazards models were used to calculate hazard ratios and 95% confidence intervals (CI) for the comparison of event rates while controlling for potential confounders. The potential confounders were selected from clinical variables and lifestyle factors associated with CKD (Table 1). Receiver operating characteristic (ROC) analyses were used to compare the predictive function of different methods in identifying individuals with Obesity, and Hanley-McNeil test was used to examine difference between area under the curves (AUCs). A p-value < 0.05 was regarded as statistically significant. The computations were performed using SPSS programs (version 11.0 J; SPSS Inc., Chicago, IL, USA).

Results

Baseline Clinical Characteristics

The upper limits of the lowest (Q1), second (Q2), and third quartiles of WheiR (Q3) were set at 0.44, 0.47 and 0.50 for males, and 0.43, 0.46 and 0.50 for females, respectively. The mean values for quartiles Q1, Q2, Q3 and Q4 of WheiR were 0.41±0.02, 0.46±0.01, 0.49±0.01 and 0.54±0.03 for males, and 0.41±0.02, 0.45±0.01, 0.48±0.01 and 0.55±0.05 for females, respectively.

Tables 2 and 3 show the participants' baseline demographic and clinical characteristics and health behaviors. There were significant associations between WheiR and age, body weight, BMI,

Table 1. Definitions of potential confounders selected from clinical variables and lifestyle factors associated with CKD.

Hypertension	Blood pressure >140/>90 mmHg and/or antihypertensives use
Diabetes mellitus	HbA1c ≥6.5%, and/or FPG ≥126 mg/dL and/or antidiabetes use
Increased LDL cholesterol	LDL cholesterol ≥140 mg/dL and/or antidyslipidemics use
Decreased HDL cholesterol	HDL cholesterol < 40 mg/dL (in men), < 50 mg/dL (in women)
Hypertriglyceridemia	TG≥150 mg/dL
Hyperuricemia	UA≥7.0 mg/dL and/or antihyperuricemics use
Preserved eGFR	eGFR≥80 ml/min/1.73 m^2
Urine occult blood	Dipstick hematuria (≥1+)

HbA1c, hemoglobin A1c; LDL cholesterol, low-density lipoprotein cholesterol; HDL cholesterol, high-density lipoprotein cholesterol; eGFR, estimated glomerular filtration rate

doi:10.1371/journal.pone.0088873.t001

SBP, DBP, ALT, AST, GGT, LDL cholesterol, HDL cholesterol, TG, FPG, HbA1c, UA, red blood cell count (RBC), hematocrit (Hct), hemoglobin (Hb), platelet counts (Plt) and leukocyte count (WBC), but there was no relationship between WheiR and Crt. Furthermore, significant positive trends for quartiles of WheiR were found for body weight, BMI, SBP, DBP, ALT, LDL cholesterol, FPG, HbA1c, UA, RBC, Hct, Hb, Plt and WBC, while significant negative trends were shown for HDL cholesterol and eGFR (all $p < 0.001$ with the polynomial contrast test). As shown in Table 3, increasing WheiR was associated with higher

Table 2. Baseline Characteristics of the Study Participants[a].

	Q1	Q2	Q3	Q4	p value
Participants, n	**1210**	**1210**	**1211**	**1210**	
Age, median (interquartile range) (year)	34 (18–67)	40 (18–66)	44 (18–63)	49 (18–67)	<0.001
Male gender	922 (76.2%)	921 (76.1%)	922 (76.1%)	921 (76.1%)	1.000
Height (cm)	168.7±7.9	167.5±7.8	166.7±7.6	165.1±8.6	<0.001
Body weight (kg)	54.7±7.7	59.2±8.8	62.8±9.1	70.5±12.6	<0.001
Body Mass Index (kg/m^2)	19.1±1.5	20.9±1.7	22.4±1.8	25.6±3.1	<0.001
Systolic blood pressure (mmHg)	109.9±11.4	113.1±12.5	116.1±13.4	120.7±13.8	<0.001
Diastolic Blood Pressure (mmHg)	68.1±8.9	71.2±9.8	73.6±10.1	76.9±10.1	<0.001
Aspartate aminotransferase (IU/L)	20.9±7.8	21.6±7.0	22.5±8.1	26.0±14.4	<0.001
Alanine aminotransferase (IU/L)	15 (3–135)	18 (4–107)	20 (5–165)	25 (5–282)	<0.001
Gamma glutamyltransferase (IU/L)	20 (7–381)	23 (7–539)	26 (7–523)	34 (7–521)	<0.001
LDL Cholesterol (mg/dL)	101.6±25.5	115.0±28.4	122.6±29.5	132.2±30.2	<0.001
Triglyceride (mg/dL)	63 (22–424)	78 (25–613)	90 (23–942)	111 (26–1155)	<0.001
HDL-cholesterol (mg/dL)	70.7±16.7	67.1±17.3	63.2±16.7	58.0±15.1	<0.001
Creatinine (mg/dL)	0.82±0.13	0.82±0.14	0.82±0.14	0.81±0.13	0.057
eGFR (ml/min/1.73 m^2)	83.2±12.3	80.3±12.6	78.2±12.6	78.3±12.2	<0.001
Fasting Plasma Glucose (mg/dL)	94.2±11.0	97.3±16.1	98.5±12.1	104.3±20.3	<0.001
HbA1c (%)	5.2±0.4	5.3±0.5	5.3±0.5	5.5±0.7	<0.001
Uric Acid (mg/dL)	5.3±1.2	5.5±1.3	5.7±1.3	5.9±1.4	<0.001
Red blood cell count (10^4/μL)	484.3±41.1	485.4±42.6	488.9±41.7	498.4±41.3	<0.001
Hemoglobin (g/dL)	14.5±1.4	14.6±1.4	14.6±1.5	15.0±1.5	<0.001
Male	15.0±1.0	15.2±0.9	15.2±1.0	15.6±1.0	<0.001
Female	12.8±1.0	12.8±1.2	12.7±1.4	13.0±1.4	0.032
Hematocrit (%)	43.9±3.6	44.2±3.7	44.3±3.9	45.1±3.9	<0.001
Platelets (10^4/μL)	23.9±4.9	24.8±5.2	25.0±5.4	25.7±6.1	<0.001
Leukocyte count (10^9/L)	5.6±1.5	5.9±1.5	5.1±1.5	6.4±1.7	<0.001

a Data are expressed as n (%) or mean ± SD or median (interquartile range)

Q1, lowest quartiles; Q2, second quartiles; Q3, third quartiles; Q4, quartiles; HDL cholesterol, high-density lipoprotein cholesterol; LDL cholesterol, low-density lipoprotein cholesterol; eGFR, estimated glomerular filtration rate; HbA1c, hemoglobin A1c

doi:10.1371/journal.pone.0088873.t002

Table 3. Clinical Characteristics of the Study Participants[a,b].

		Q1	Q2	Q3	Q4	p value
Urine occult blood		55 (4.5%)	61 (5.0%)	44 (3.6%)	59 (4.9%)	0.345
Hypertension		34 (2.8%)	66 (5.5%)	105 (8.7%)	221 (18.3%)	<0.001
Diabetes mellitus		9 (0.7%)	28 (2.3%)	24 (2.0%)	102 (10.8%)	<0.001
Increased LDL cholesterol		104 (8.6%)	229 (18.9%)	329 (27.2%)	482 (39.8%)	<0.001
Decreased HDL cholesterol		28 (2.3%)	36 (3.0%)	59 (4.9%)	104 (8.6%)	<0.001
Hypertriglyceridemia		29 (2.4%)	128 (10.6%)	202 (16.7%)	351 (29.0%)	<0.001
Preserved eGFR		684 (56.5%)	538 (44.5%)	473 (39.1%)	435 (36.0%)	<0.001
Hyperuricemia		1101 (91.5%)	1039 (85.9%)	999 (82.5%)	924 (76.4%)	<0.001
Smoking status						<0.001
	Never smokers	747 (61.7%)	681 (56.3%)	652 (53.8%)	645 (53.3%)	
	Former smokers	175 (14.5%)	201 (16.6%)	252 (20.8%)	268 (22.2%)	
	Current Smokers	288 (23.8%)	328 (27.1%)	307 (25.4%)	297 (24.5%)	
Alcohol drinking behavior						<0.001
	Non/Rare	523 (43.2%)	438 (36.2%)	450 (37.2%)	507 (41.9%)	
	Sometimes	488 (40.3%)	473 (39.1%)	456 (37.7%)	430 (35.5%)	
	Every day	199 (16.4%)	299 (24.7%)	305 (25.2%)	273 (22.6%)	
Regular exercise		256 (21.2%)	278 (23.0%)	260 (21.5%)	270 (22.3%)	0.696

a Data are expressed as n (%).
b Definitions of these confounding factors are shown in Table 1.
WheiR, waist to height ratio; Q1, lowest quartiles; Q2, second quartiles; Q3, third quartiles; Q4, quartiles; LDL cholesterol, low-density lipoprotein cholesterol; HDL cholesterol, High-density lipoprotein cholesterol; eGFR, estimated glomerular filtration rate.
doi:10.1371/journal.pone.0088873.t003

proportion of hypertension, diabetes mellitus, increased LDL cholesterol, decreased HDL cholesterol, hypertriglyceridemia, and hyperuricemia (all $p < 0.001$ with Kendall's tau-b), while the proportion of urine occult blood and regular exercise did not associate with quartiles of WheiR.

The Incidence of CKD in Relation to Quartiles of WheiR

A total of 384 (7.9%) participants including 300 men and 84 women received a new diagnosis of CKD during the study period, and 45, 79, 122 and 138 diagnoses were received in Q1, Q2, Q3 and Q4 of WheiR, respectively. The overall incidence of CKD was 29.7 per 1000 person-years. A graded relationship existed between WheiR and the incidence of CKD (Table 4).

In the unadjusted analysis, Cox proportional-hazards models revealed that the risk of CKD rose with each increasing quartile of WheiR. In a test for interaction between the quartiles of WheiR and follow-up time, there was no violation of the proportional-hazards assumption. In the multivariable analysis, the significant graded association between WheiR and the hazards ratio for CKD persisted after adjustment for age, gender, smoking status, alcohol drinking behavior, regular exercise, hypertension, increased LDL cholesterol, decreased HDL cholesterol, hypertriglyceridemia, hyperuricemia, urine occult blood, hemoglobin and preserved eGFR at baseline (Table 4). However, after further adjustment for BMI, WheiR was no longer a risk factor for the incidence of CKD.

Because significant negative trend was also shown for eGFR at baseline though the quartiles of WheiR (Table 2), we next performed further assessment for the relationship among eGFR, WheiR and a risk of CKD to eliminate the effect of baseline eGFR level. We divided the study participants into gender-, and eGFR at baseline (eGFR $\geq$80 ml/min/1.73 m^2 or <80 ml/min/1.73 m^2) - adjusted quartiles of the distribution of WheiR, and then, we calculated the hazards ratios for the incidence of CKD. In participants with decreased eGFR (eGFR < 80 ml/min/1.73 m^2), the unadjusted hazards ratio (HR) (95% confidence interval (CI)) for the incidence of CKD was 1.00 (reference), 1.67 (1.17, 2.39, $p = 0.005$), 2.64 (1.76, 3.45, $p < 0.001$) and 2.39 (1.70, 3.36, $p < 0.001$) though the quartiles of re-classified WheiR, respectively. After adjustment for age, gender, smoking status, alcohol drinking behavior, regular exercise, hypertension, increased LDL cholesterol, decreased HDL cholesterol, hypertriglyceridemia, hyperuricemia, urine occult blood and hemoglobin, this significant graded association between re-classified WheiR and the hazards ratio for CKD persisted (adjusted HR (95%CI); 1.00 (reference), 1.41 (0.98, 2.03, $p = 0.064$), 1.81 (1.28, 2.58, $p = 0.001$) and 1.61 (1.12, 2.34, $p = 0.011$) though the quartiles of re-classified WheiR, respectively). However, in participant with preserved eGFR (eGFR $\geq$80 ml/min/1.73 m^2), these associations were not observed (adjusted HR (95%CI); 1.00 (reference), 0.71 (0.21, 2.37, $p = 0.575$), 0.81 (0.25, 2.59, $p = 0.721$) and 2.12 (0.73, 6.16, $p = 0.036$) though the quartiles of re-classified WheiR, respectively).

The Incidence of Low eGFR and Proteinuria in Relation to Quartiles of WheiR

Table 5 shows the unadjusted and adjusted hazard ratios for low eGFR and proteinuria. In the unadjusted model, there was a significant graded association between WheiR and the incidence of both low eGFR and proteinuria, and these relationships persisted after adjustment for age, gender, smoking status, alcohol drinking behavior, regular exercise, hypertension, increased LDL cholesterol, decreased HDL cholesterol, hypertriglyceridemia, hyperuricemia, urine occult blood, hemoglobin and preserved eGFR at baseline. After further adjustment for BMI, WheiR associated with the incidence of neither proteinuria nor low eGFR.

Table 4. Incidence of CKD in Relation to Quartiles of Waist to height ratio (WheiR).

Quartile of WheiR	Incidence (/1000 person-years)	Unadjusted hazards ratio(95% CI)	p value	Adjusted hazards ratio (95% CI)[a]	p value	Adjusted hazards ratio (95% CI)[b]	p value
Q1	13.7	(reference)		(reference)		(reference)	
Q2	24.2	1.75 (1.29, 2.52)	0.003	1.23 (0.85, 1.78)	0.275	0.99 (0.65, 0.66)	0.963
Q3	37.9	2.78 (1.98, 3.91)	<0.001	1.59 (1.11, 2.26)	0.011	1.15 (0.73, 1.80)	0.547
Q4	47.3	3.31 (2.36, 4.65)	<0.001	1.62 (1.13, 2.32)	0.009	1.14 (0.67, 1.91)	0.633
p for trend			<0.001		0.004		0.464

a (model 2) Adjusted for age, gender, smoking status, alcohol drinking behavior, regular exercise, hypertension, increased low-density lipoprotein cholesterol, decreased High-density lipoprotein cholesterol, hypertriglyceridemia, hyperuricemia, diabetes mellitus, urine occult blood, hemoglobin and preserved eGFR at baseline.
b (model 3) Adjusted for model 2 plus body mass index. Cox proportional-hazards models were used to calculate hazard ratios and 95% confidence intervals. Definitions of these confounding factors are shown in Table 1.
WheiR, waist to height ratio; CI, confidence interval, Q1, lowest quartiles; Q2, second quartiles; Q3, third quartiles; Q4, highest quartiles
doi:10.1371/journal.pone.0088873.t004

Table 5. Incidence of Proteinuria and Low eGFR in Relation to Quartiles of Waist to height ratio (WheiR).

	Quartile of WheiR	Unadjusted hazards ratio (95% CI)	p value	Adjusted hazards ratio (95% CI)[a]	p value	Adjusted hazards ratio (95% CI)[b]	p value
Low eGFR	Q1		(reference)		(reference)		(reference)
	Q2	2.00 (1.35, 2.94)	0.001	1.33 (0.90, 1.98)	0.152	1.05 (0.68, 1.34)	0.82
	Q3	3.10 (2.15, 4.47)	<0.001	1.64 (1.12, 2.39)	0.011	1.15 (0.71, 1.85)	0.579
	Q4	3.36 (2.34, 4.85)	<0.001	1.54 (1.04, 2.27)	0.03	1.04 (0.60, 1.81)	0.881
	p for trend		<0.001		0.029		0.811
Proteinuria	Q1	(reference)	(reference)	(reference)			
	Q2	0.56 (0.16, 1.91)	0.356	0.57 (0.18, 2.00)	0.387	0.50 (0.13, 1.98)	0.323
	Q3	1.16 (0.42, 3.19)	0.778	1.21 (0.42, 3.49)	0.724	0.89 (0.20, 3.95)	0.88
	Q4	3.28 (1.40, 7.67)	0.006	2.68 (1.01, 7.10)	0.047	1.58 (0.29, 8.57)	0.594
	p for trend		0.001		0.011		0.366

a (model 2) Adjusted for age, gender, smoking status, alcohol drinking behavior, regular exercise, hypertension, increased low-density lipoprotein cholesterol, decreased high-density lipoprotein cholesterol, hypertriglyceridemia, hyperuricemia, diabetes mellitus, urine occult blood, hemoglobin and preserved eGFR at baseline.
b (model 3) Adjusted for model 2 plus body mass index. Cox proportional-hazards models were used to calculate hazard ratios and 95% confidence intervals. Definitions of these confounding factors are shown in Table 1.
WheiR, waist to height ratio; CI, confidence interval; Q1, lowest quartiles; Q2, second quartiles; Q3, third quartiles; Q4, highest quartiles.
doi:10.1371/journal.pone.0088873.t005

Table 6. Incidence of CKD in Relation to Quartiles of Waist to height ratio (WheiR) Stratified by Gender.

Gender	Quartile of WheiR	Unadjusted hazards ratio (95% CI)	p value	Adjusted hazards ratio (95% CI)a	p value	Adjusted hazards ratio (95% CI)b	p value
Male	Q1	(reference)	(reference)	(reference)			
	Q2	1.42 (0.96, 2.11)	0.081	0.94 (0.63, 1.41)	0.781	0.64 (0.40, 1.03)	0.063
	Q3	2.18 (1.52, 3.14)	<0.001	1.18 (0.80, 1.73)	0.412	0.70 (0.42, 1.17)	0.168
	Q4	2.73 (1.91, 3.90)	<0.001	1.25 (0.84, 1.86)	0.269	0.71 (0.39, 1.30)	0.267
	p for trend		<0.001		0.111		0.746
Female	Q1	(reference)	(reference)				
	Q2	6.40 (1.90, 21.63)	0.003	5.31 (1.55, 18.16)	0.008	5.06 (1.45, 17.59)	0.011
	Q3	11.42 (3.49, 37.36)	<0.001	9.24 (2.76, 30.91)	<0.001	8.12 (2.25, 29.75)	0.001
	Q4	11.49 (3.51, 36.42)	<0.001	7.18 (2.12, 24.19)	0.002	5.77 (1.41, 23.62)	0.015
	p for trend		<0.001		0.001		0.041

a Adjusted for age, smoking status, alcohol drinking behavior, regular exercise, hypertension, increased low-density lipoprotein cholesterol, decreased high-density lipoprotein cholesterol, hypertriglyceridemia, hyperuricemia, diabetes mellitus, urine occult blood, hemoglobin and preserved eGFR at baseline.
b (model 3) Adjusted for model 2 plus body mass index. Cox proportional-hazards models were used to calculate hazard ratios and 95% confidence intervals. Definitions of these confounding factors are shown in Table 1.
WheiR, waist to height ratio; CI, confidence interval; Q1, lowest quartiles; Q2, second quartiles; Q3, third quartiles; Q4, highest quartiles
doi:10.1371/journal.pone.0088873.t006

Gender Differences in the Relationship between the Incidence of CKD and Quartiles of WheiR

Next, we investigated the association between gender, WheiR and the incidence of CKD. Table 6 shows the unadjusted and adjusted hazard ratios for CKD for males and females. In the unadjusted analysis, a graded relationship existed between WheiR and the risk of CKD in both males and females. However, after adjusting for potential confounders including BMI, WheiR was significantly associated with the incidence of CKD in females, whereas it was not significant in males.

Comparison of the Predictive Values of CKD in Each Surrogate Maker of Obesity

We also investigated the relationship between other markers of obesity including WC and BMI, and the incidence of CKD. To assess these relations, we divided the study participants into gender-adjusted quartiles of the distribution of WC and BMI. Table 7 shows the unadjusted and adjusted hazards ratios for CKD in each surrogate marker. In the unadjusted analysis, a graded relationship existed between both WC and BMI, and the risk of CKD. In the multivariable analyses, the significant graded association between these markers and the hazards ratio for CKD persisted after adjustment for potential confounders.

We also investigated the association between gender, WC, BMI and the incidence of CKD. In the unadjusted analyses, a graded relationship existed between each WC and BMI, and the risk of CKD in both gender. However, after adjusting for potential confounders, WC was not associated with the incidence of CKD in males.

The Performance of the WheiR for Predicting CKD

Finally, we performed the ROC analyses to examine which surrogate markers of body fat including WheiR, WC and BMI were superior predictors of the incidence of CKD. As shown in figure 1A, The AUC of WheiR was higher than those of both WC and BMI (WheiR, WC and BMI: 0.628 (95% Confidence interval; 0.601–0.655), 0.611 (0.584, 0.638), $p = 0.015$, and 0.607 (0.579, 0.635), $p = 0.012$, respectively). Figure 1B and 1C shows the gender difference of predicting values for the incidence of CKD. The AUC of WheiR was similar to those of both WC and BMI (WheiR, WC and BMI: 0.619 (0.587, 0.650), 0.604 (0.572, 0.635), $p = 0.117$, and 0.604 (0.572, 0.636), $p = 0.052$, respectively.) in male gender (Figure 1B), and the AUC of WheiR was also similar to those of both WC and BMI (WheiR, WC and BMI: 0.660 (0.610, 0.710), 0.656 (0.604, 0.708), $p = 0.060$, and 0.628 (0.572, 0.685), $p = 0.604$, respectively) in female gender (Figure 1C).

Discussion

In this study, we found that the WheiR was an independent predictor for the incidence of CKD in the Japanese workers who participated. A graded relationship existed between quartiles of WheiR and the incidence of CKD. Compared with the lowest quartile, the incidence of CKD was 1.6 times higher in the highest quartile. WheiR had a strong predictive value for the incidence of both proteinuria and low eGFR. However, these relationships were abolished after adjustment BMI. There was a significant gender difference in the relationship between CKD and WheiR. After subdivision according to gender, the relationship between WheiR and the incidence of CKD was statistically significant in the unadjusted model in both genders. However, after adjusting for potential confounders including BMI, WheiR was significantly associated with the incidence of CKD in females, whereas it was not significant in males.

It is well-established that overall and central obesity are associated with cardiovascular risk factors such as hyperglycemia, diabetes, hypertension, dyslipidemia and metabolic syndrome [21,22]. WheiR, WC and BMI could similarly predict cardiometabolic risk factors [22]. Most public health literature is focused on the use of BMI to identify obesity. However, BMI does not distinguish between muscle and fat, visceral and subcutaneous fat, or peripheral and central adiposity. A previous study indicated that WC strongly correlated with visceral fat as measured by computed tomography [23]. Furthermore, because height is also one of the factors that influences fat accumulation and distribution, WheiR might be a more accurate way to track fat distribution and accumulation than weight circumference [18]. Thus, we used WheiR as an index for central obesity.

Table 7. Comparison of the Predictive Values of CKD in Each Surrogate Maker of Obesity.

Gender	Marker	Quartile of WheiR	Unadjusted hazards ratio (95% CI)	p value	Adjusted hazards ratio (95% CI)[a]	p value
Overall	Waist circumference	Q1	(reference)		(reference)	
		Q2	1.91 (1.33, 2.73)	<0.001	1.41 (0.98, 2.02)	0.068
		Q3	2.47 (1.75, 3.48)	<0.001	1.47 (1.03, 2.09)	0.033
		Q4	3.06 (2.19, 4.30)	<0.001	1.67 (1.16, 2.39)	0.006
		p for trend		<0.001		0.009
	Body mass index	Q1	(reference)		(reference)	
		Q2	2.08 (1.46, 2.97)	<0.001	1.58 (1.10, 2.25)	0.013
		Q3	2.66 (1.88, 3.75)	<0.001	1.80 (1.27, 2.57)	0.001
		Q4	2.90 (2.07, 4.08)	<0.001	1.79 (1.25, 2.56)	0.001
		p for trend		<0.001		0.003
Males	Waist circumference	Q1	(reference)		(reference)	
		Q2	1.67 (1.12, 2.48)	0.012	1.14 (0.77, 1.72)	0.507
		Q3	2.33 (1.61, 3.38)	<0.001	1.34 (0.90, 1.97)	0.139
		Q4	2.57 (1.78, 3.73)	<0.001	1.38 (0.92, 2.07)	0.122
		p for trend		<0.001		0.088
	Body mass index	Q1	(reference)		(reference)	
		Q2	2.25 (1.51, 3.35)	<0.001	1.68 (1.12, 2.52)	0.012
		Q3	2.63 (1.78, 3.90)	<0.001	1.78 (1.19, 2.67)	0.005
		Q4	2.82 (2.82, 4.15)	<0.001	1.79 (1.18, 2.70)	0.006
		p for trend		<0.001		0.019
Females	Waist circumference	Q1	(reference)		(reference)	
		Q2	3.45 (1.40, 8.47)	0.007	2.99 (1.21, 7.39)	0.018
		Q3	3.29 (1.31, 8.24)	0.011	2.43 (0.96, 6.15)	0.061
		Q4	6.27 (2.60, 14.89)	<0.001	3.93 (1.61, 9.60)	0.003
		p for trend	<0.001		0.006	
	Body mass index	Q1	(reference)		(reference)	
		Q2	1.47 (0.66, 3.28)	0.344	1.39 (0.60, 3.00)	0.481
		Q3	2.75 (1.34, 5.63)	0.006	2.33 (1.12, 4.86)	0.023
		Q4	3.19 (1.56, 6.35)	0.001	2.32 (1.11, 4.87)	0.025
		p for trend		<0.001		0.009

a Adjusted for age, smoking status, alcohol drinking behavior, regular exercise, hypertension, increased low-density lipoprotein cholesterol, decreased high-density lipoprotein cholesterol, hypertriglyceridemia, hyperuricemia, diabetes mellitus, urine occult blood, hemoglobin and preserved eGFR at baseline. Cox proportional-hazards models were used to calculate hazard ratios and 95% confidence intervals. Definitions of these confounding factors are shown in Table 1.
CI, confidence interval; Q1, lowest quartiles; Q2, second quartiles; Q3, third quartiles; Q4, highest quartiles.
doi:10.1371/journal.pone.0088873.t007

Obesity and metabolic syndrome are known as independent risk factors for CKD [24,25]. In previous studies, obesity has been implicated in the development focal segmental glomerulosclerosis and glomerulomegaly [26,27]. Visceral adipose tissue secretes inflammatory cytokines such as interleukin-6 and tumor necrosis factor α, which are associated with both obesity-related glomerulopathy and metabolic syndrome [28–32]. It is not clear if it is central obesity or the related cardiometabolic risk factors that initiate renal injury. In the current study, the association between the WheiR and CKD remained robust even after adjusting for confounding factors, including cardiometabolic risk factors. This result suggested that the risk for CKD was not solely attributable to metabolic syndrome, which is consistent with a previous study that showed WheiR was significantly associated with CKD, independent of hypertension and diabetes [33].

In our results, WheiR was an independent predictor for the incidence of CKD in participants with eGFR < 80 mL/min/1.73 m^2, however, this association was not significant in participants with eGFR ≥80 mL/min/1.73 m^2. We speculated that this result was affected by inclusion of participants at different degree of proteinuria. Although several participants were diabetic, dyslipidemic and hypertensive in our study, we did not evaluate the microalbuminuria and had no information concerning the presence of proteinuria or kidney diseases without the results of self-administrated questionnaire before the study began. The lack of these data partially affected our results of the association between WheiR and the future appearance of a renal dysfunction.

Our results indicated the WheiR was an independent risk factor for the incidence of both low eGFR and proteinuria. However, the endpoint for the incident of proteinuria might lack the statistical and biological power, because p values were at the threshold of significance. Dipstick urinalysis might not be a reliable screening method for proteinuria. Previous study reported that the sensitivity, specificity and positive and negative predictive values

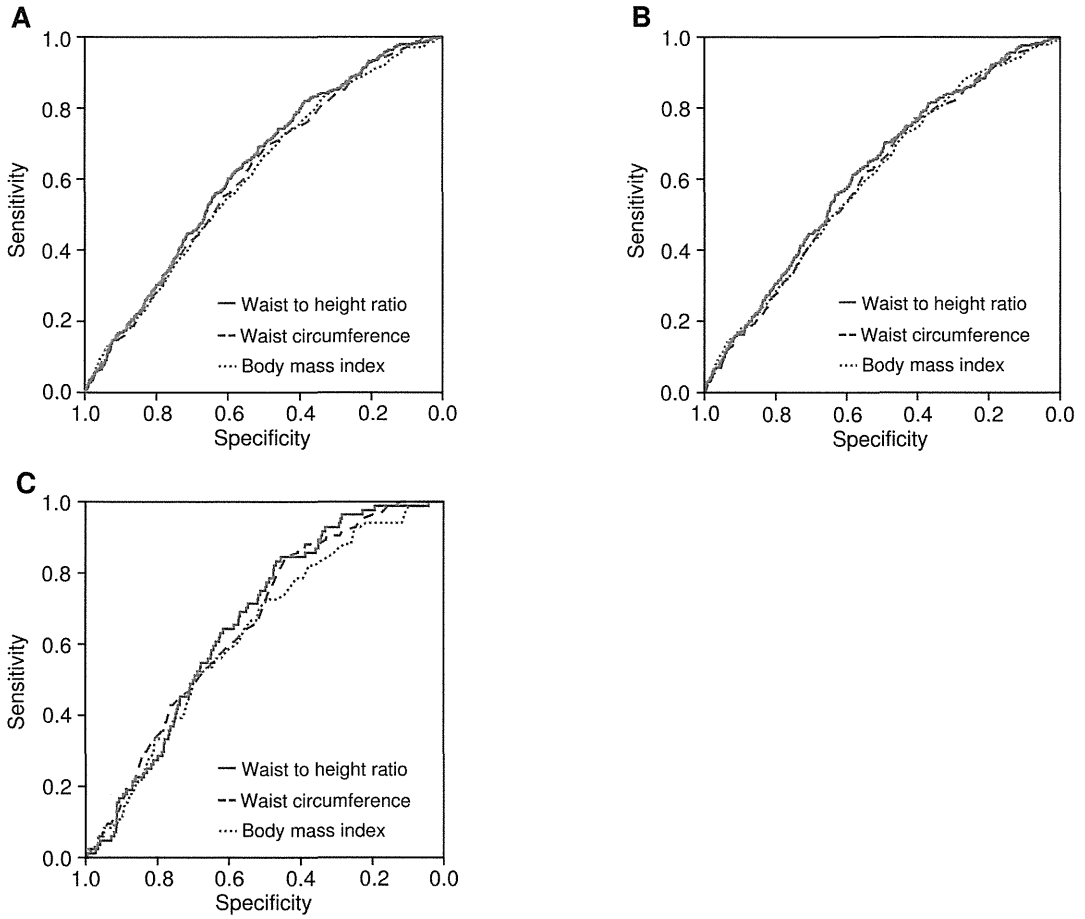

Figure 1. Receiver operating characteristic analyses describing the predictive value of each surrogate marker of obesity. (A) The area under the receiver operating characteristic curve (AUC) of waist to height ratio (WheiR), body mass index (BMI) and waist circumference (WC) were calculated as 0.628 (95% Confidence interval; 0.601–0.655), 0.611 (0.584, 0.638), and 0.607 (0.579, 0.635), respectively in all study participants. (B) and (C) Participants were stratified by gender. The AUCs of WheiR, BMI and WC were 0.619 (0.587, 0.650), 0.604 (0.572, 0.635), and 0.604 (0.572, 0.636), respectively, in male gender (B), and 0.660 (0.610, 0.710), 0.656 (0.604, 0.708), and 0.628 (0.572, 0.685), respectively, in female gender (C).
doi:10.1371/journal.pone.0088873.g001

of the dipstick test for detection of protein were 80.0%, 95.0%, 22.2% and 99.6% [34].

We found gender differences in the association between WheiR and the risk of CKD. Previous studies have reported that WheiR was more frequently associated with renal injury in females than males [33,35]. Although it remains unclear how gender influences the correlation between WheiR and CKD, several hypotheses have proposed. First, the lack of an association between the WheiR and CKD in males suggested that the risk factors might be different between males and females and that factors other than central obesity might be more important in males. Second, anemia might contribute to the progression of CKD, especially in females. Because hypoxia can be exacerbated by lower hemoglobin levels, anemia might have a role in the progression of CKD. In our participants, the hemoglobin levels were lower values in females than those in males through the quartiles of WheiR (Table 2). However, in our study, after adjustment for potential confounders including hemoglobin, WheiR was still an independent predictor for CKD. Finally, another possibility is that sex hormones might have a role in the interaction with this association. Further studies are necessary to elucidate the mechanism by which gender differences have an influence on these relationships.

In this study, we also evaluated the predictive values of other markers of obesity. Our results indicated that BMI also had a strong predictive value as same as WheiR (Table 4, 7). Interestingly, as shown in Table 6, WheiR was still an independent risk factor for the incidence of CKD after adjustment for potential confounder including BMI in only females. This finding supported the gender differences in the association between WheiR and the risk of CKD.

The current study has several limitations. First, we did not evaluate the changes in WheiR in individual participants during the study period. Second, self-reported information regarding daily regular exercise, alcohol intake and smoking status is prone to underreporting, and misreporting could be a source of bias. Third, we did not investigate whether participants underwent kidney biopsy, thus, the etiology of the CKD associated with WheiR was not identified. However, the proportion of hypertensive and diabetes in participant with developing CKD were higher than those in participants without developing CKD (data not shown). These associations suggested that some of the etiology of CKD might be glomerular sclerosis and/or diabetic nephropathy. Fourth, we could not completely exclude the participants who had any infections, malignances or other peculiar disorders, because our self-administered standardized questionnaire did not require

filling out about these information. Finally, there might be selection bias related to the healthy worker effect.

In conclusion, WheiR, which is one of the markers of central obesity, has the potential to be a useful surrogate marker for predicting the future development of CKD. There was a significant gender difference in the relationship between CKD and WheiR. Further study is needed to clarify the efficacy of interventions reducing the WheiR to decline the risk of CKD.

Acknowledgments

We are indebted to Dr. Sachiko Miyakawa and Dr. Akio Hakamata for editorial help. The authors thank the study participants for their time and dedication to the study.

Author Contributions

Conceived and designed the experiments: KO. Performed the experiments: KO MY IM YM AU. Analyzed the data: KO. Wrote the paper: KO. Revised the manuscript: AU HW.

References

1. Go AS, Chertow GM, Fan D, McCulloch CE, Hsu CY (2004) Chronic kidney disease and the risks of death, cardiovascular events, and hospitalization. N Engl J Med 351: 1296–1305.
2. Hallan SI, Dahl K, Oien CM, Grootendorst DC, Aasberg A, et al. (2006) Screening strategies for chronic kidney disease in the general population: follow-up of cross sectional health survey. BMJ 333: 1047.
3. Hooi LS, Ong LM, Ahmad G, Bavanandan S, Ahmad NA, et al. (2013) A population-based study measuring the prevalence of chronic kidney disease among adults in West Malaysia. Kidney Int 84: 1034–1040.
4. Kearns B, Gallagher H, de Lusignan S (2013) Predicting the prevalence of chronic kidney disease in the English population: a cross-sectional study. BMC Nephrol 14: 49–59.
5. Zhang L, Wang F, Wang L, Wang W, Liu B, et al. (2012) Prevalence of chronic kidney disease in China: a cross-sectional survey. Lancet 379: 815–822.
6. Imai E, Horio M, Watanabe T, Iseki K, Yamagata K, et al. (2009) Prevalence of chronic kidney disease in the Japanese general population. Clin Exp Nephrol 13: 621–630.
7. Coresh J, Selvin E, Stevens LA, Manzi J, Kusek JW, et al. (2007) Prevalence of chronic kidney disease in the United States. JAMA 298: 2038–2047.
8. Nagata M, Ninomiya T, Doi Y, Yonemoto K, Kubo M, et al. (2010) Trends in the prevalence of chronic kidney disease and its risk factors in a general Japanese population: the Hisayama Study. Nephrol Dial Transplant 25: 2557–2564.
9. Grams ME, Juraschek SP, Selvin E, Foster MC, Inker LA, et al. (2013) Trends in the Prevalence of Reduced GFR in the United States: A Comparison of Creatinine- and Cystatin C-Based Estimates. Am J Kidney Dis. 62: 253–260.
10. Brosius FC 3rd, Hostetter TH, Kelepouris E, Mitsnefes MM, Moe SM, et al. (2006) Detection of chronic kidney disease in patients with or at increased risk of cardiovascular disease: a science advisory from the American Heart Association Kidney And Cardiovascular Disease Council; the Councils on High Blood Pressure Research, Cardiovascular Disease in the Young, and Epidemiology and Prevention; and the Quality of Care and Outcomes Research Interdisciplinary Working Group: developed in collaboration with the National Kidney Foundation. Circulation 114: 1083–1087.
11. Heerspink HL, de Zeeuw D (2013) Novel drugs and intervention strategies for the treatment of chronic kidney disease. Br J Clin Pharmacol 76: 536–550.
12. Govindarajan G, Whaley-Connell A, Mugo M, Stump C, Sowers JR (2005) The cardiometabolic syndrome as a cardiovascular risk factor. Am J Med Sci 330: 311–318.
13. Kuk JL, Katzmarzyk PT, Nichaman MZ, Church TS, Blair SN, et al. (2006) Visceral fat is an independent predictor of all-cause mortality in men. Obesity (Silver Spring) 14: 336–341.
14. Manolopoulos KN, Karpe F, Frayn KN (2010) Gluteofemoral body fat as a determinant of metabolic health. Int J Obes (Lond) 34: 949–959.
15. Liu J, Fox CS, Hickson D, Bidulescu A, Carr JJ, et al. (2011) Fatty liver, abdominal visceral fat, and cardiometabolic risk factors: the Jackson Heart Study. Arterioscler Thromb Vasc Biol 31: 2715–2722.
16. Katzmarzyk PT, Heymsfield SB, Bouchard C (2013) Clinical utility of visceral adipose tissue for the identification of cardiometabolic risk in white and African American adults. Am J Clin Nutr 97: 480–486.
17. Rothney MP, Catapano AL, Xia J, Wacker WK, Tidone C, et al. (2013) Abdominal visceral fat measurement using dual-energy X-ray: Association with cardiometabolic risk factors. Obesity (Silver Spring) 21: 1798–1802.
18. Hsieh SD, Yoshinaga H, Muto T (2003) Waist-to-height ratio, a simple and practical index for assessing central fat distribution and metabolic risk in Japanese men and women. Int J Obes Relat Metab Disord 27: 610–616.
19. Ashwell M, Gunn P, Gibson S (2012) Waist-to-height ratio is a better screening tool than waist circumference and BMI for adult cardiometabolic risk factors: systematic review and meta-analysis. Obes Rev 13: 275–286.
20. Matsuo S, Imai E, Horio M, Yasuda Y, Tomita K, et al. (2009) Revised equations for estimated GFR from serum creatinine in Japan. Am J Kidney Dis 53: 982–992.
21. Chiba Y, Saitoh S, Takagi S, Ohnishi H, Katoh N, et al. (2007) Relationship between visceral fat and cardiovascular disease risk factors: the Tanno and Sobetsu study. Hypertens Res 30: 229–236.
22. Liu Y, Tong G, Tong W, Lu L, Qin X (2011) Can body mass index, waist circumference, waist-hip ratio and waist-height ratio predict the presence of multiple metabolic risk factors in Chinese subjects? BMC Public Health 11: 11–35.
23. Sanches FM, Avesani CM, Kamimura MA, Lemos MM, Axelsson J, et al. (2008) Waist circumference and visceral fat in CKD: a cross-sectional study. Am J Kidney Dis 52: 66–73.
24. Tanaka H, Shiohira Y, Uezu Y, Higa A, Iseki K (2006) Metabolic syndrome and chronic kidney disease in Okinawa, Japan. Kidney Int 69: 369–374.
25. Kurella M, Lo JC, Chertow GM (2005) Metabolic syndrome and the risk for chronic kidney disease among nondiabetic adults. J Am Soc Nephrol 16: 2134–2140.
26. Verani RR (1992) Obesity-associated focal segmental glomerulosclerosis: pathological features of the lesion and relationship with cardiomegaly and hyperlipidemia. Am J Kidney Dis 20: 629–634.
27. Weisinger JR, Kempson RL, Eldridge FL, Swenson RS (1974) The nephrotic syndrome: a complication of massive obesity. Ann Intern Med 81: 440–447.
28. Wu Y, Liu Z, Xiang Z, Zeng C, Chen Z, et al. (2006) Obesity-related glomerulopathy: insights from gene expression profiles of the glomeruli derived from renal biopsy samples. Endocrinology 147: 44–50.
29. Wisse BE (2004) The inflammatory syndrome: the role of adipose tissue cytokines in metabolic disorders linked to obesity. J Am Soc Nephrol 15: 2792–2800.
30. Hotamisligil GS, Arner P, Caro JF, Atkinson RL, Spiegelman BM (1995) Increased adipose tissue expression of tumor necrosis factor-alpha in human obesity and insulin resistance. J Clin Invest 95: 2409–2415.
31. Hotamisligil GS, Spiegelman BM (1994) Tumor necrosis factor alpha: a key component of the obesity-diabetes link. Diabetes 43: 1271–1278.
32. Pickup JC, Mattock MB, Chusney GD, Burt D (1997) NIDDM as a disease of the innate immune system: association of acute-phase reactants and interleukin-6 with metabolic syndrome X. Diabetologia 40: 1286–1292.
33. Lin CH, Chou CY, Lin CC, Huang CC, Liu CS, et al. (2007) Waist-to-height ratio is the best index of obesity in association with chronic kidney disease. Nutrition 23: 788–793.
34. Zamanzad B (2009) Accuracy of dipstick urinalysis as a screening method for detection of glucose, protein, nitrites and blood. East Mediterr Health J 15: 1323–1328.
35. Tseng CH (2005) Waist-to-height ratio is independently and better associated with urinary albumin excretion rate than waist circumference or waist-to-hip ratio in chinese adult type 2 diabetic women but not men. Diabetes Care 28: 2249–2251.

Beta Cell Telomere Attrition in Diabetes: Inverse Correlation Between HbA1c and Telomere Length

Yoshiaki Tamura,[1] Naotaka Izumiyama-Shimomura,[2] Yoshiyuki Kimbara,[1] Ken-ichi Nakamura,[2] Naoshi Ishikawa,[2] Junko Aida,[2] Yuko Chiba,[1] Seijiro Mori,[1] Tomio Arai,[3] Toru Aizawa,[4] Atsushi Araki,[1] Kaiyo Takubo,[2] and Hideki Ito[1]

Departments of [1]Diabetes, Metabolism, and Endocrinology and [3]Pathology, Tokyo Metropolitan Geriatric Hospital, Tokyo, Japan; [2]Research Team for Geriatric Pathology and Department of Pathology, Tokyo Metropolitan Geriatric Hospital and Institute of Gerontology, Tokyo, Japan; and [4]Diabetes Center, Aizawa Hospital, Matsumoto, Nagano, Japan

Context: Although accelerated β cell telomere shortening may be associated with diabetes which shows a dramatically increased incidence with aging, β cell telomere length in diabetes has never been explored.

Objective: The objective of the present study was to examine telomere length in the β cells of patients with diabetes.

Design and patients: We determined telomere length in β and α cells of pancreases obtained at autopsy from 47 patients with type 2 diabetes and 51 controls, all over 60 years of age.

Main outcome measure: The normalized telomere-centromere ratio (NTCR), an index of telomere length, was determined for β (NTCRβ) and α (NTCRα) cells by quantitative fluorescence *in situ* hybridization.

Results: The NTCRβ was reduced by 27±25% and NTCRα by 15± 27% in the patients with diabetes relative to the controls ($P<0.01$ for both). Importantly, the degree of shortening was significantly ($P<0.01$) greater in β cells than in α cells. The histogram of NTCR distribution was significantly skewed to the left in the patients with diabetes relative to the controls for both β and α cells, indicating preferential depletion of longer-telomere islet cells. HbA1c was negatively correlated with β cell telomere length, and the telomeres were significantly shorter in patients who had used hypoglycemic agents than in those who had not.

Conclusion: The telomeres of β cells are shortened in patients with type 2 diabetes. There may be a vicious cycle involving β cell telomere attrition and sustained hyperglycemia.

The worldwide incidence of type 2 diabetes has increased rapidly in the past two decades. Diabetes causes microand macrovascular complications which degrade the quality of life (QOL) of affected patients and impose a huge economic burden on global health systems (1). The prevalence of type 2 diabetes increases with age, and the number of elderly patients with diabetes has been increasing explosively. In patients with type 2 diabetes, both increased insulin resistance and attenuated insulin secretion from pancreatic β cells are common features (2, 3). In association with aging, insulin resistance increases with a reduction of lean body mass and a relative increase of fat mass. At the same time, the mass of pancreatic β cells decreases with aging in relation to their diminished proliferative capacity and depressed cell cycle activity (4–8). This strongly suggests that the accelerated loss of β cells may contribute to impaired insulin secretion and the development and progression of type 2 diabetes in humans.

Telomeres are repetitive G-rich DNA sequences located at the ends of linear eukaryotic chromosomes, and play a

ISSN Print 0021-972X ISSN Online 1945-7197
Printed in U.S.A.

Received January 24, 2014. Accepted April 8, 2014.

Abbreviations:

pivotal role in preventing genomic instability (9). It is thought that telomeric repeats protect chromosomes against degeneration, reconstruction, fusion, and loss (10). With the exception of immortal, carcinomatous and germ cells, the telomeres of all cells shorten with each cell division due to end-replication attrition (10, 11), and for this reason telomere length has been used as a marker of cellular senescence: cells stop dividing when telomeres shorten to a critical length (12).

Telomere shortening has been observed in the peripheral blood cells of patients with type 2 diabetes (13–15), and is associated with increased prevalence of diabetic complications (16, 17) and mortality (18). In the pancreases of mice with shortened telomeres due to lack of the *telomerase RNA component*, islet size is reduced and the replication capacity of the β cells is limited (19). In addition, telomere shortening has been reported to compromise β-cell signaling and survival in mice (20). However, telomere length in the β cells of patients with type 2 diabetes has never been evaluated. Against this background, in the present study we analyzed the telomere length of β cells in patients with type 2 diabetes.

Materials and Methods

Specimens of pancreatic tail tissue were obtained from 47 consecutively autopsied patients with type 2 diabetes and 51 consecutively autopsied control patients without diabetes. The patients in both groups had common diseases such as malignancies, stroke, coronary heart disease (CHD) and pneumonia (see below). All of the patients were Japanese, over 60 years of age, and had died at Tokyo Metropolitan Geriatric Hospital. We adopted the maximum HbA1c in the past as an index of the degree of hyperglycemia in each patient. Diabetes was diagnosed if the maximum recorded HbA1c was 6.5% or over, or if the patient had a history of treatment with hypoglycemic agents (HA), including oral hypoglycemic agents and insulin. We defined 'nondiabetic' as a past maximum HbA1c of $< 6.5\%$ and no medical history or diagnosis of diabetes mellitus and treatment with antidiabetic drugs. The onset of diabetes had not been abrupt in any of the patients, and type 2 diabetes had been diagnosed by experienced diabetologists. Patients with type 1 diabetes, or diabetes with endocrine disorders or pancreatic diseases, were excluded, as were those with pancreatic cancer. BMI was calculated from the height and weight measured at autopsy. For serum creatinine, triglyceride, total cholesterol and HDL cholesterol, the data obtained upon last hospitalization were used, and if no admission data were available, the most recent data obtained before admission were used. The estimated glomerular filtration rate (eGFR) was calculated using the equation: eGFR (mL/min/1.73 m^2) = 194 · serum creatinine$^{-1.094}$ · age$^{-0.287}$ · 0.739 (if female) (21), where the unit of creatinine is mg/100 mL.

The paraffin-embedded pancreatic tail samples were sliced into sections for telomere length determination using the immunofluorescence method. The sections used were examined histopathologically by specialists in anatomical and surgical pathology (J.A., T.Arai and K.T., who were unaware of the clinical data) and sections with marked accumulation of inflammatory cells and/or autolysis were not included in this study. Approval for the study was obtained from the ethics committee of Tokyo Metropolitan Geriatric Hospital and Institute of Gerontology.

Telomere lengths of the cells were measured by the quantitative fluorescence in situ hybridization (FISH) (Q-FISH) method, as described previously (22–24). Briefly, Cy3-labeled PNA probes for the telomere and fluorescein isothiocyanate (FITC)-labeled probes for the centromere were hybridized on each sample slide, and the respective signal intensities were determined. Because there is no guarantee that the entire nucleus is captured within a tissue section, the total corrected telomere signal (integrated optical density) for each nucleus is further normalized by the corresponding integrated optical density of the centromere. We have previously verified in a fluorescence flow study (data not shown) that the mean optical density of our centromere probe was constant among human blood cells from individuals of various age groups and cultured fibroblasts, TIG-1. Pancreatic α cells and β cells were distinguished using a guinea pig anti-insulin antibody (No.N1542, Dako, Glostrup, Denmark), a guinea pig antiglucagon antibody (No.M182, Takara Bio Inc., Shiga, Japan), and a secondary goat antiguinea pig antibody labeled with Cy-5 (ab6567, Abcam plc, Cambridge, UK) after FISH. At least 100 (106–304) α and β cells were analyzed for each case. As an index of telomere length, we first calculated the telomere:centromere ratio (TCR), and subsequently carried out normalization of the TCR to obtain the normalized TCR (NTCR) by dividing the TCR of pancreatic cells by that of TIG-1, stained simultaneously on the same slide, as described previously (22–24).

The median NTCR values for β cells (NTCRβ) and α cells (NTCRα) were used as a representative value for each cell type in individual patients. Fractional shortening of NTCR in a patient with diabetes relative to the controls was calculated as follows: (1-(NCTR of a patient with diabetes / mean value of NTCR for the controls)) x 100 (%)

Mann-Whitney U test, paired *t* test, Spearman's rank correlation test, multiple regression analysis and histo-